GEOPHYSICS, VOL. 78, NO. 4 (JULY-AUGUST 2013); P. T113–T132, 22 FIGS., 8 TABLES.
10.1190/GEO2012-0480.1

Globally optimal finite-difference schemes based on least squares

Yang Liu[1]

ABSTRACT

Spatial finite-difference (FD) coefficients are usually determined by the Taylor-series expansion (TE) or optimization methods. The former can provide high accuracy on a smaller wavenumber or frequency zone, and the latter can give moderate accuracy on a larger zone. Present optimization methods applied to calculate FD coefficients are generally gradient-like or global optimization-like algorithms, and thus iterations are involved. They are more computationally expensive, and sometimes the global solution may not be found. I examined second-order spatial derivatives and computed the optimized spatial FD coefficients over the given wavenumber range using the least-squares (LS) method. The results indicated that the FD accuracy increased with increasing operator length and decreasing wavenumber range. Therefore, for the given error and operator length, globally optimal spatial FD coefficients can be easily obtained. Some optimal FD coefficients were given. I developed schemes to obtain optimized LS-based spatial FD coefficients by minimizing the relative error of space-domain dispersion relation for second-order derivatives and time-space-domain dispersion relation for the acoustic wave equation. I discovered that minimizing the relative error of the space-domain dispersion relation provides less phase velocity error for small wavenumbers, compared to minimizing the absolute error. I also found that minimizing the relative error of the time-space-domain dispersion relation can reduce relative errors of phase velocity. Accuracy analysis demonstrated the correctness and advantage of schemes. I gave three examples of 2D acoustic FD modeling for a homogeneous, a large velocity-contrast, and a heterogeneous model, respectively. LS-based spatial FD operators have variable lengths for different velocities. Modeling examples demonstrated that the proposed LS-based FD scheme can maintain the same modeling precision while using a shorter spatial FD operator length, thus reducing the computation cost relative to conventional TE-based FD schemes, particularly for the higher order.

INTRODUCTION

Finite-difference (FD) methods have been widely applied in numerically solving wave equations for their small computational costs and easy implementation (e.g., Kelly et al., 1976; Virieux, 1984, 1986; Levander, 1988; Lele, 1992; Tam and Webb, 1993; Moczo et al., 2000, 2011; Etgen and O'Brien, 2007; Bansal and Sen, 2008; Hestholm, 2009). Many studies focus on designing FD stencils and determining FD coefficients to improve the accuracy, the efficiency, or both (e.g., Dablain, 1986; Jastram and Behle, 1993; Saenger et al., 2000; Takeuchi and Geller, 2000; Finkelstein and Kastner, 2007; JafarGandomi and Takenaka, 2009; Liu and Sen, 2011a; Song and Fomel, 2011; Leandro et al., 2012). FD coefficients can be calculated by directly expanding functions at grids using Taylor series (e.g., Dablain, 1986; Fornberg, 1987; Liu et al., 1998; Liu and Wei, 2008; Du et al., 2009) or by recursions (Fornberg, 1998), etc. However, it is more flexible and thus popular to calculate FD coefficients based on minimizing dispersion relations such as wavenumber dispersion relations and velocity dispersion relations. FD dispersion relations generally are functions of sine or cosine.

There are mainly two kinds of methods to calculate FD coefficients based on dispersion relations. The first kind is the Taylor series expansion-based method. This method uses Taylor-series expansion (TE) to expand trigonometric functions in FD dispersion relations into polynomials. The polynomial coefficients are used to obtain FD coefficients (e.g., Liu and Sen, 2009a, 2009b, 2009c; Chu and Stoffa, 2012a).

The second kind is an optimization-based method. This method usually calculates optimized FD coefficients under the conditions of

Manuscript received by the Editor 13 November 2012; revised manuscript received 10 February 2013; published online 24 June 2013.
[1]China University of Petroleum, State Key Laboratory of Petroleum Resources and Prospecting and CNPC Key Laboratory of Geophysical Prospecting, Beijing, China. E-mail: wliuyang@vip.sina.com.

the given bandwidth and operator length. It commonly adopts gradient-like algorithms such as linear or nonlinear least squares (LS) to minimize FD dispersion relations over the wavenumber or frequency range to obtain FD coefficients (e.g., Robertsson et al., 1994; Shan, 2009; Kosloff et al., 2010; Zhou and Zhang, 2011; Chen, 2012). To satisfy the specified accuracy over the wavenumber or frequency range, Holberg (1987) states that it is necessary to maximize the wavenumber or frequency range under the conditions of the given accuracy and the given operator length. Kindelan et al. (1990) adopt a variant of Newton's method to solve the problem. Global optimization algorithms such as simulated annealing have been reported to try to obtain the best optimized FD coefficients and bandwidth (Zhang and Yao, 2012). Optimized FD coefficients can be determined by truncating the spatial convolution series of the pseudospectral method (e.g., Zhou and Greenhalgh, 1992; Igel et al., 1995). Liu and Sen (2009d, 2011b) find that there are negligibly small values in the TE-based high-order FD coefficients, and they proposed the truncated FD method to decrease the operator length while maintaining the same approximate accuracy. Truncated FD coefficients can also be determined by using scaled binomial windows, and thus optimized FD operators with enhanced dispersion properties can be obtained (Chu and Stoffa, 2012b).

Of these methods, the TE-based method has the lowest computational expense for calculating FD coefficients, and it usually provides the higher accuracy over the smaller wavenumber or frequency range. The present local optimization based method and the truncation-based method have moderate computational costs yet may not obtain globally optimized FD coefficients. The present global optimization based method has the highest computational expense but sometimes may not find the best optimization solution. A possible approach is, through using variable substitution, constraints, or approximations, to make the multiextreme optimization problem into a convex optimization problem and the nonlinear optimization problem into a linear problem. When the optimization problem becomes convex and linear, the solution can be directly obtained by LS without iterations.

In this paper, I propose a method to obtain globally optimal FD coefficients over the maximum bandwidth for second-order spatial derivatives under the conditions of the specified accuracy and operator length based on minimizing the absolute error of space-domain dispersion relation by LS. I further develop methods to obtain optimal spatial FD coefficients by the LS method of minimizing the relative error of space-domain dispersion relation for second-order derivatives and the relative error of time-space-domain dispersion relation for the acoustic wave equation. Accuracy analysis and modeling experiments demonstrate their accuracies and advantages. In addition, I develop LS-based algorithms to obtain optimal FD coefficients for two FD modeling problems. Dispersion analyses also show that two proposed algorithms provide fewer dispersion errors than two published algorithms.

A GLOBALLY OPTIMAL FD SCHEME FOR SECOND-ORDER DERIVATIVES

FD coefficients calculated by LS

I start from the FD stencil for second-order derivatives.

An FD operator involved $2M+1$ points for a function $p(x)$ is expressed as

$$\frac{\partial^2 p}{\partial x^2} \approx \frac{1}{h^2}\left(c_0 p(x) + \sum_{m=1}^{M} c_m (p(x+mh) + p(x-mh))\right), \tag{1}$$

where x is a real variable, h is a small positive value, c_m are FD coefficients.

Let

$$p(x+mh) = p_0 e^{\mathrm{i}k(x+mh)}, \tag{2}$$

where p_0 is a constant value, $\mathrm{i} = \sqrt{-1}$, and k represents the wavenumber. Substitute equation 2 into 1 and obtain

$$-k^2 \approx \frac{1}{h^2}\left(c_0 + 2\sum_{m=1}^{M} c_m \cos(mkh)\right). \tag{3}$$

When $k = 0$, equation 3 becomes

$$c_0 + 2\sum_{m=1}^{M} c_m = 0. \tag{4}$$

Then equation 3 becomes

$$f(\beta) \approx \sum_{m=1}^{M} c_m \varphi_m(\beta), \tag{5}$$

where

$$f(\beta) = \beta^2, \qquad \varphi_m(\beta) = 2(1-\cos(m\beta)), \tag{6}$$

$\beta = kh$. β only ranges from 0 to π because kh equals π at the Nyquist frequency.

When the TE-based strategy is used to calculate FD coefficients $(2M)$th-order accuracy can be obtained. Generally, TE-based FD coefficients can provide accurate derivatives along the interval of β. Outside this interval, the accuracy of the calculated derivatives usually decreases with the increase of β (e.g., Liu and Sen, 2009a).

Usually, the FD error is expected to be small on a given interval $[0, b]$ $(b > 0)$. The expected error for any given interval decreases as the FD operator length increases. Therefore, it is possible to find the shortest length of the FD operator for the given interval and the expected error.

First, I outline the method to calculate the optimal FD coefficients through minimizing the square error over the given interval $[0, b]$ as follows:

$$E = \int_0^b \left(\sum_{m=1}^{M} c_m \varphi_m(\beta) - f(\beta)\right)^2 d\beta. \tag{7}$$

Because $\varphi_1(\beta), \varphi_2(\beta), \ldots, \varphi_M(\beta)$ are independent on the interval $[0, b]$, the LS solution of minimizing the error of equation 7 exists, and it is unique and globally optimal. Then, optimal c_m can be obtained by solving the following equations using LS:

$$\sum_{m=1}^{M}\left(\int_0^b \varphi_m(\beta)\varphi_n(\beta)d\beta\right)c_m = \int_0^b f(\beta)\varphi_n(\beta)d\beta,$$
$$(n = 1, 2, \ldots, M). \tag{8}$$

Accuracy analysis

I compare the FD accuracy of the TE-based method (TEM) and the LS-based method (LSM). TE-based FD coefficients for second-order derivatives can be obtained by the following formulas (e.g., Liu and Sen, 2009a):

$$c_m = \frac{(-1)^{m+1}}{m^2}\prod_{1\le n\le M, n\ne m}\left|\frac{n^2}{n^2-m^2}\right|,$$
$$(m = 1, 2, \ldots, M) \tag{9}$$

and equation 4.

To examine the accuracy, I calculate the variation of the root-mean-square (rms) error ε_r and the maximum error ε_{max} with b and M using the following formulas:

$$\varepsilon_{rms} = \sqrt{\frac{1}{b}\int_0^b \varepsilon^2(\beta)d\beta}, \tag{10}$$

$$\varepsilon_{max} = \max_{\beta\in[0,b]}|\varepsilon(\beta)|, \tag{11}$$

where

$$\varepsilon(\beta) = \sum_{m=1}^{M} c_m\varphi_m(\beta) - f(\beta). \tag{12}$$

Figure 1 shows variations of $\log_{10}(\varepsilon_{rms})$ and $\log_{10}(\varepsilon_{max})$ with b for different M by the TEM and the LSM, respectively. From the top

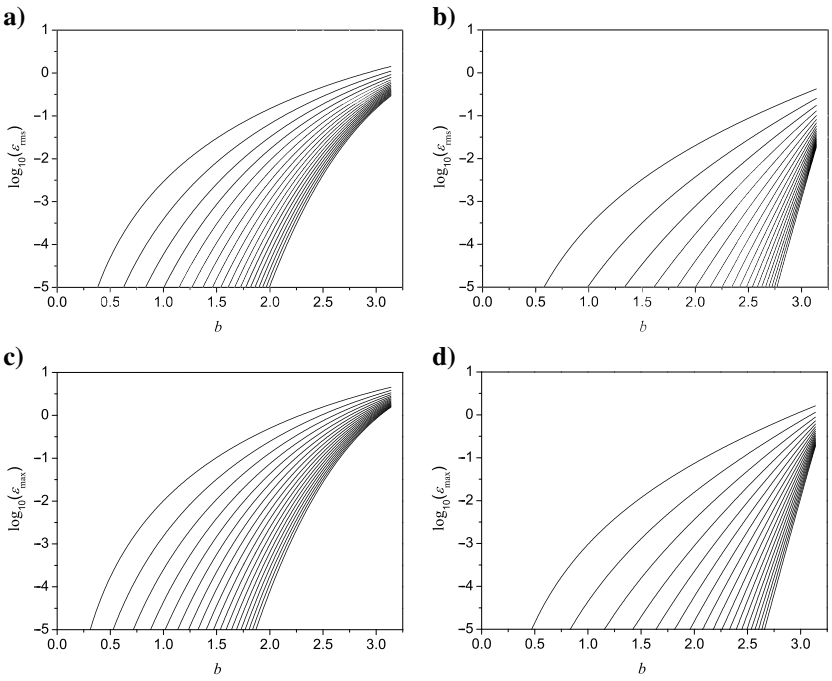

Figure 1. Variations of $\log_{10}(\varepsilon_{rms})$ and $\log_{10}(\varepsilon_{max})$ with b for different M by the TEM and the LSM of minimizing the absolute error of space-domain dispersion relation, respectively. Variations of $\log_{10}(\varepsilon_{rms})$ with b are shown (a) by the TEM and (b) by the LSM. Variations of $\log_{10}(\varepsilon_{max})$ with b are shown (c) by the TEM and (d) by the LSM. From top to bottom, lines are from $M = 2, 3, \ldots, 20$, respectively.

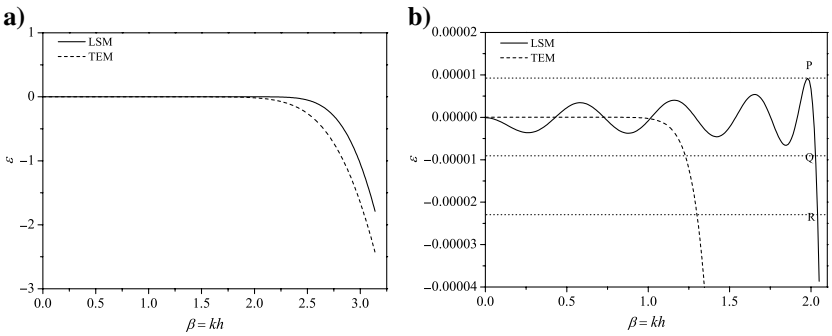

Figure 2. Variations of ε with β in (a) and its magnification in (b) by the TEM and the LSM of minimizing the absolute error of the space-domain dispersion relation, respectively. $M = 8$. For the LSM, $b = 2.04$ is used in equation 8 together with 6 to calculate c_m ($m = 0, 1, \ldots, 8$), and their values are $-0.3164237E+1$, $0.1877867E+1$, $-0.3876708E+0$, $0.1241696E+0$, $-0.4328630E-1$, $0.1439029E-1$, $-0.4154609E-2$, $0.9258541E-3$, and $-0.1219996E-3$, respectively. At points R and Q, $\beta = b$ and $\beta = B$. At points P and Q, $|\varepsilon|$ have the same value.

Table 1. The B values for different M and maximum error η from the TEM and the LSM of minimizing the absolute error of space-domain dispersion relation, respectively ($\varepsilon_{\max} < \eta$ in the interval $[0,B]$).

	B					
	$\eta = 10^{-3}$		$\eta = 10^{-4}$		$\eta = 10^{-5}$	
M	TEM	LSM	TEM	LSM	TEM	LSM
2	0.67	1.11	0.45	0.76	0.31	0.52
3	0.94	1.57	0.70	1.20	0.52	0.91
4	1.15	1.89	0.90	1.53	0.71	1.24
5	1.32	2.12	1.07	1.79	0.87	1.50
6	1.45	2.28	1.21	1.99	1.01	1.72
7	1.56	2.41	1.32	2.14	1.13	1.89
8	1.65	2.50	1.42	2.26	1.23	2.02
9	1.73	2.58	1.50	2.35	1.32	2.14
10	1.79	2.64	1.58	2.43	1.40	2.23
11	1.85	2.69	1.64	2.49	1.47	2.32
12	1.91	2.73	1.70	2.55	1.53	2.39
13	1.95	2.76	1.75	2.60	1.58	2.44
14	2.00	2.79	1.80	2.65	1.63	2.49
15	2.03	2.82	1.84	2.68	1.68	2.54
16	2.07	2.84	1.88	2.71	1.72	2.58
17	2.10	2.86	1.92	2.74	1.76	2.61
18	2.13	2.87	1.95	2.76	1.80	2.64
19	2.16	2.89	1.98	2.78	1.83	2.66
20	2.18	2.91	2.01	2.80	1.86	2.69
30	2.36	3.00	2.22	2.92	2.09	2.84
40	2.47	3.04	2.34	2.98	2.23	2.92
50	2.55	3.06	2.43	3.01	2.33	2.97

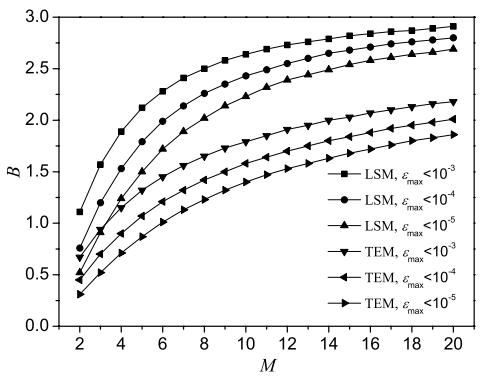

Figure 3. Variations of B with M for different maximum errors η by the TEM and the LSM of minimizing the absolute error of space-domain dispersion relation, respectively. In the interval $[0, B]$, $\varepsilon_{\max} < \eta$ is satisfied.

to the bottom of the figure, the lines represent $M = 2, 3, \ldots, 20$, respectively. This figure suggests that

- For fixed M, the error increases with increasing b.
- For fixed b, the error decreases with increasing M.
- For the same error, the LSM has a larger wavenumber range than the TEM.

Therefore, one can find the unique b for any given M that provides the given maximum error η. Thus, FD coefficients can be obtained using equation 8 together with 6. This solution is globally optimal.

A globally optimal FD scheme for second-order derivatives

To obtain optimal FD coefficients, I first study the characteristics of $\varepsilon(\beta)$. As an example, Figure 2 displays $\varepsilon(\beta)$ by the TEM and the LSM, respectively, where $M = 8$. The value $b = 2.04$ is used in equation 8 together with 6 to calculate FD coefficients c_m. In the interval $[0, b]$, ε fluctuates around zero. In the interval $[b, \pi]$,

Table 2. The b values used to calculate FD coefficients by the LSM of minimizing the absolute error of space-domain dispersion relation for different M and maximum error η ($\varepsilon_{\max} < \eta$ in the interval $[0,B]$, B is shown in Table 1).

	b		
M	$\eta = 10^{-3}$	$\eta = 10^{-4}$	$\eta = 10^{-5}$
2	1.16	0.79	0.54
3	1.61	1.23	0.93
4	1.93	1.56	1.26
5	2.15	1.82	1.52
6	2.31	2.01	1.74
7	2.44	2.16	1.91
8	2.53	2.28	2.04
9	2.60	2.37	2.16
10	2.66	2.45	2.25
11	2.71	2.51	2.33
12	2.75	2.57	2.40
13	2.78	2.62	2.45
14	2.81	2.66	2.50
15	2.84	2.69	2.55
16	2.86	2.72	2.59
17	2.88	2.75	2.62
18	2.89	2.77	2.65
19	2.91	2.79	2.67
20	2.92	2.81	2.70
30	3.01	2.93	2.85
40	3.05	2.99	2.93
50	3.07	3.02	2.98

absolute values of ε increase with increasing β. The curve of $|\varepsilon(\beta)|$ from the LSM has several peaks, which have very close values. Among these peaks, the maximum value ε_P, ε at point P shown in Figure 2, is less than $\varepsilon_R = |\varepsilon(b)|$, ε at point R shown in Figure 2. There is a point Q shown in Figure 2: $\beta = B$ and $|\varepsilon| = \varepsilon_P$ for this point. Similar characteristics can be found from other curves of $\varepsilon(\beta)$ for different M and b, for instance, curves shown in later figures. The maximum value in the interval $[0, B]$ is ε_P. Because $\varepsilon_P = \varepsilon_Q < \varepsilon_R$ and $B < b$, I use b to calculate c_m but find ε_{max} in the interval $[0, B]$. In other words, because the maximum absolute error in the given interval $[0, b_Q]$ when using $b = b_Q$ to calculate c_m is greater than that using $b = b_R$, to get the smaller maximum absolute error in $[0, b_Q]$, I adopt $b = b_R$ instead of $b = b_Q$ to calculate c_m.

For the given maximum error $\eta = 10^{-3}$, 10^{-4}, 10^{-5}, I obtain B values for different M from the TEM and the LSM shown in Table 1 and Figure 3, respectively, where $\varepsilon_{max} < \eta$ is satisfied in the interval $[0, B]$ and b used to calculate c_m are shown in Table 2. Table 1 and Figure 3 suggest that the LSM provides much wider zone than the TEM for the same η and M. For example, when $M = 8$ and $\eta = 10^{-5}$, the zone with this accuracy from the TEM is $[0, 1.23]$ but the zone from the LSM broadens about two-thirds and reaches $[0, 2.02]$.

Table 3 lists FD coefficients from the LSM when $\eta = 10^{-4}$. Figure 4 shows variations of ε with β for different M from the TEM and the LSM, respectively. One can see that the LSM significantly widens the range with the given maximum error $\eta = 10^{-4}$ for the same M, compared to the TEM.

GLOBALLY OPTIMAL FD SCHEMES FOR ACOUSTIC WAVE EQUATIONS

Optimal FD coefficients are usually designed by minimizing relative wavenumber, frequency, or phase velocity errors in numerical wave equations (e.g., Holberg, 1987; Kindelan et al., 1990; Lele, 1992; Chen, 2012). In this section, based on the space-domain and the time-space-domain dispersion relations, respectively, I design optimal spatial FD coefficients by minimizing the relative error of dispersion relations for the acoustic wave equation. The steps obtaining FD coefficients are similar as described above.

A globally optimal FD scheme based on space-domain dispersion relation

In formula 7, let

$$\varphi_m(\beta) = 2(1 - \cos(m\beta))/\beta^2, \qquad f(\beta) = 1. \tag{13}$$

Then, formula 7 represents the relative error. Therefore, based on the space-domain dispersion relation, FD coefficients for second-order spatial derivatives can be obtained by minimizing formula 7 in which $\varphi_m(\beta)$ and $f(\beta)$ are replaced by equation 13. Note that minimizing the relative error of the space-domain dispersion relation can provide fewer phase velocity errors of acoustic FD modeling for small wavenumbers, compared to minimizing the absolute error, which has been proved in Appendix A.

Table 3. Optimized FD coefficients by the LSM of minimizing the absolute error of space-domain dispersion relation for the maximum error $\eta = 10^{-4}$.

c	$M = 2$	$M = 3$	$M = 4$	$M = 5$	
c_0	$-0.2552812E+1$	$-0.2817830E+1$	$-0.2968111E+1$	$-0.3061625E+1$	
c_1	$0.1369074E+1$	$0.1573661E+1$	$0.1700010E+1$	$0.1782836E+1$	
c_2	$-0.9266816E-1$	$-0.1820268E+0$	$-0.2554615E+0$	$-0.3124513E+0$	
c_3		$0.1728053E-1$	$0.4445392E-1$	$0.7379487E-1$	
c_4			$-0.4946851E-2$	$-0.1532122E-1$	
c_5				$0.1954439E-2$	
c	$M = 6$	$M = 7$	$M = 8$	$M = 9$	$M = 10$
c_0	$-0.3120756E+1$	$-0.3160790E+1$	$-0.3188824E+1$	$-0.3208344E+1$	$-0.3223372E+1$
c_1	$0.1837023E+1$	$0.1874503E+1$	$0.1901160E+1$	$0.1919909E+1$	$0.1934461E+1$
c_2	$-0.3538895E+0$	$-0.3845794E+0$	$-0.4074304E+0$	$-0.4240446E+0$	$-0.4372298E+0$
c_3	$0.9978343E-1$	$0.1215162E+0$	$0.1390909E+0$	$0.1526043E+0$	$0.1637716E+0$
c_4	$-0.2815486E-1$	$-0.4121749E-1$	$-0.5318775E-1$	$-0.6322328E-1$	$-0.7201005E-1$
c_5	$0.6556587E-2$	$0.1295522E-1$	$0.2004823E-1$	$0.2676005E-1$	$0.3315012E-1$
c_6	$-0.9405699E-3$	$-0.3313813E-2$	$-0.6828249E-2$	$-0.1080739E-1$	$-0.1504262E-1$
c_7		$0.5310053E-3$	$0.1895771E-2$	$0.3907747E-2$	$0.6430730E-2$
c_8			$-0.3369052E-3$	$-0.1158024E-2$	$-0.2458744E-2$
c_9				$0.2240247E-3$	$0.7777024E-3$
c_{10}					$-0.1641995E-3$

Figure 5 displays variations of $\log_{10}(\varepsilon_{\max})$ with b for different M by the TEM and the LSM of minimizing the relative error of space-domain dispersion relation, respectively. This figure also demonstrates that the error increases with increasing b and decreasing M, and the LSM has the larger wavenumber range than the TEM for the same maximum error. Figure 6 shows $\varepsilon(\beta)$ by the TEM and the LSM of minimizing the relative error of space-domain dispersion relation, respectively, where $M = 8$. $b = 2.10$ is adopted in equation 8 together with equation 13 to calculate FD coefficients c_m. Figures 6 and 2 have similar characteristics.

Similarly, for the given maximum error $\eta = 10^{-4}, 10^{-5}, 10^{-6}$, I get B values for different M from the TEM and the LSM shown in Table 4 and Figure 7, respectively, where $\varepsilon_{\max} < \eta$ is satisfied in the interval $[0, B]$ and b used to calculate c_m are shown in Table 5. From Table 4 and Figure 7, it can be seen that the LSM gives a much wider zone than the TEM for the same η and M. Table 6 gives FD coefficients from the LSM when $\eta = 10^{-5}$. Figure 8 displays variations of ε with β for different M from the TEM and the LSM, respectively. The figure suggests that the LSM greatly enlarges the range with the given maximum error $\eta = 10^{-5}$ for the same M, compared to the TEM.

A nearly globally optimal FD scheme based on 1D time-space-domain dispersion relation

For 1D acoustic FD modeling, time-space-domain dispersion-relation-based spatial FD coefficients can be determined by using the following formula (Liu and Sen, 2009c):

$$\sum_{m=1}^{M} c_m(1-\cos(mkh)) \approx r^{-2}(1-\cos(rkh)), \tag{14}$$

where $r = v\tau/h$, v is the velocity, τ is the time step, and h is the grid size. Using TE for equation 14, FD coefficients can be obtained as follows (Liu and Sen, 2009c):

$$c_m = \frac{(-1)^{m+1}}{m^2} \prod_{1\le n\le M, n\ne m} \left|\frac{n^2-r^2}{n^2-m^2}\right|, \quad (m = 1, 2, \ldots, M). \tag{15}$$

For 1D acoustic FD modeling, the relative error of phase velocity ξ is defined as follows (Liu and Sen, 2009c, 2011a):

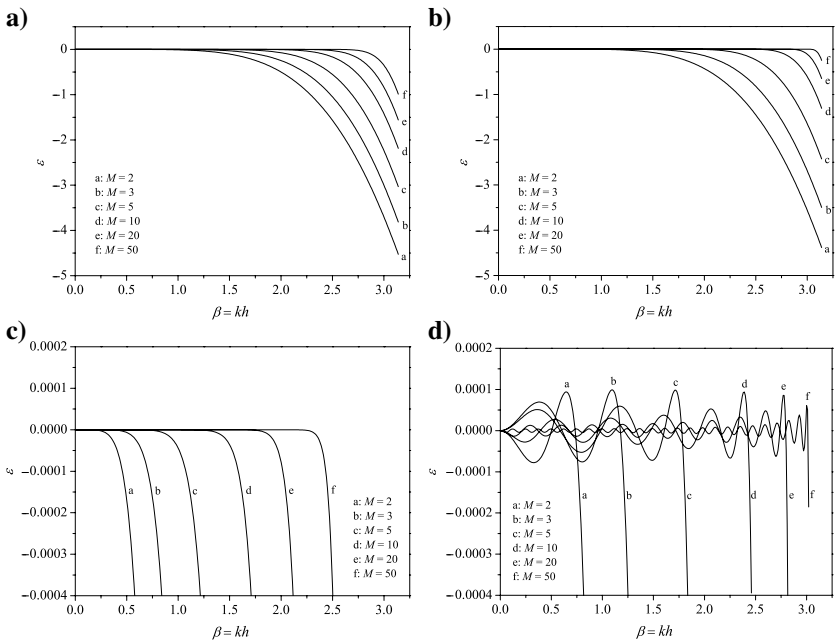

Figure 4. Variations of ε with β for different M by the TEM and the LSM of minimizing the absolute error of space-domain dispersion relation, respectively. (a) Is by the TEM, and (b) is by the LSM. (c) Is a magnification of (a), and (d) is a magnification of (b). FD coefficients of the LSM with maximum error $\eta = 10^{-4}$ used in the figure ($M = 2, 3, 5, 10$) are listed in Table 3.

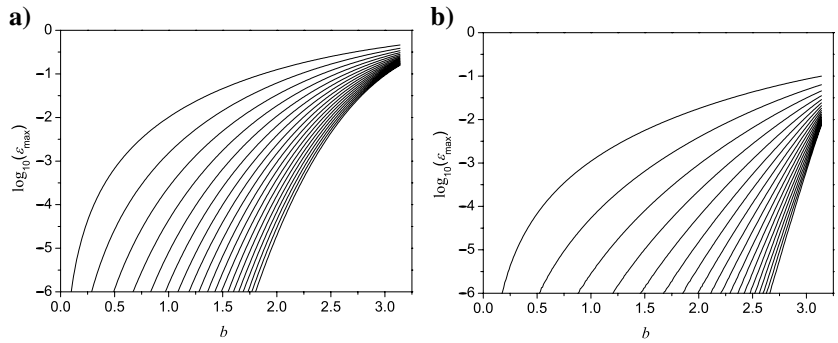

Figure 5. Variations of $\log_{10}(\varepsilon_{\max})$ with b for different M by (a) the TEM and (b) the LSM of minimizing the relative error of space-domain dispersion relation, respectively. From top to bottom, lines are from $M = 2, 3, \ldots, 20$, respectively. Maximum values are calculated in the interval $[0, B]$.

$$\xi = \frac{v_{\mathrm{FD}}}{v} - 1 = \frac{2}{r\beta}\sin^{-1}\sqrt{\frac{r^2}{2}\sum_{m=1}^{M}(1-\cos(m\beta))c_m} - 1. \tag{16}$$

Directly minimizing ξ leads to a nonlinear problem. To avoid this problem, I minimize the relative error between the left item and the right item of equation 14. FD coefficients can then be derived by minimizing formula 7 using the following $\varphi_m(\beta)$ and $f(\beta)$:

$$\varphi_m(\beta) = \frac{1-\cos(m\beta)}{r^{-2}(1-\cos(r\beta))}, \qquad f(\beta) = 1. \tag{17}$$

To test the accuracy, I calculate the variation of the maximum error $\xi_{\max}$ with b and M by using

$$\xi_{\max} = \max_{\beta\in[0,b]}|\xi(\beta)|. \tag{18}$$

Figure 9 shows variations of $\log_{10}(\xi_{\max})$ with b for different M by the TEM and the LSM of minimizing the relative error of 1D time-space-domain dispersion relation, respectively. This figure also suggests that the error increases with increasing b and decreasing M, and the LSM has the larger wavenumber range than the TEM for the same maximum error. Figure 10 displays $\xi(\beta)$ by the TEM and the LSM of minimizing the relative error of 1D time-space-domain dispersion relation, respectively, where $M = 8$. The value $b = 2.21$ is used in equation 8 together with 17 to calculate FD coefficients c_m. Figures 10 and 2 have similar characteristics.

I obtain B values for different M from the TEM and the LSM shown in Figure 11 for the given maximum error $\eta = 10^{-4}$, 10^{-5}, 10^{-6} where $r = 0.5$, $\xi_{\max} < \eta$ is satisfied in the interval $[0, B]$ and b is used to calculate c_m. This figure suggests that the LSM provides a much wider zone than the TEM for the same η and M. Figure 12 shows variations of ξ with β for different M from the TEM and the LSM, respectively. It can be seen that the LSM greatly broadens the range with the maximum error $\eta = 10^{-5}$ for the same M, compared to the TEM.

Appendix B illustrates why minimizing the relative error of the time-space-domain dispersion relation can lead to small relative error of phase velocity. Note that the LS-based solution of FD coefficients is exactly globally optimal for minimizing the relative error of the time-space-domain dispersion relation. However, it is not exactly but nearly globally optimal for minimizing relative error of phase velocity. Actually, I calculate the optimal solution of minimizing relative error of phase velocity by the conjugate gradient method using the LS-based solution as the starting one, and results shows that the optimal solution is almost the same as the LS-based solution when the given maximum error is small.

Table 4. The B values for different M and maximum error η from the TEM and the LSM of minimizing the relative error of space-domain dispersion relation, respectively ($\varepsilon_{\max} < \eta$ in the interval $[0,B]$).

	B					
	$\eta = 10^{-4}$		$\eta = 10^{-5}$		$\eta = 10^{-6}$	
M	TEM	LSM	TEM	LSM	TEM	LSM
2	0.30	0.51	0.17	0.27	0.09	0.15
3	0.62	1.06	0.42	0.72	0.28	0.50
4	0.88	1.49	0.65	1.13	0.49	0.86
5	1.09	1.81	0.85	1.46	0.67	1.18
6	1.25	2.05	1.01	1.71	0.83	1.43
7	1.38	2.22	1.15	1.92	0.96	1.65
8	1.50	2.35	1.27	2.08	1.08	1.83
9	1.59	2.45	1.37	2.20	1.18	1.97
10	1.67	2.54	1.45	2.30	1.27	2.09
11	1.74	2.60	1.53	2.39	1.35	2.19
12	1.80	2.65	1.60	2.45	1.42	2.28
13	1.86	2.70	1.66	2.51	1.48	2.35
14	1.91	2.73	1.71	2.56	1.54	2.41
15	1.95	2.77	1.76	2.62	1.59	2.46
16	1.99	2.79	1.80	2.65	1.64	2.51
17	2.03	2.82	1.84	2.69	1.68	2.55
18	2.06	2.84	1.88	2.71	1.73	2.58
19	2.09	2.86	1.92	2.74	1.76	2.61
20	2.12	2.87	1.95	2.76	1.80	2.64
30	2.32	2.98	2.17	2.90	2.04	2.82
40	2.44	3.03	2.31	2.97	2.20	2.91
50	2.52	3.05	2.40	3.01	2.30	2.96

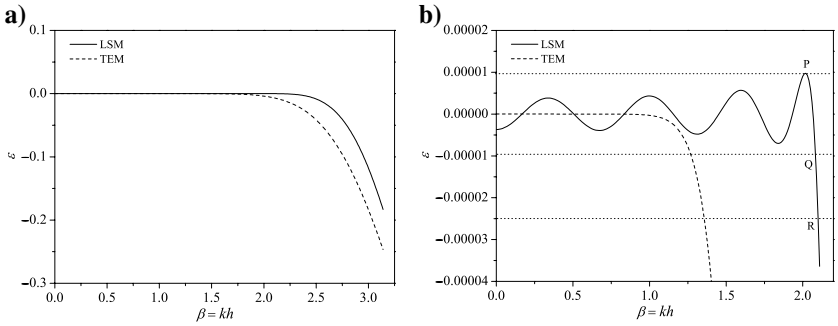

Figure 6. Variations of ε with β (a) and its magnification (b) by the TEM and the LSM of minimizing the relative error of space-domain dispersion relation, respectively. $M = 8$. For the LSM, $b = 2.10$ is used in equation 8 together with 13 to calculate c_m ($m = 0, 1, \ldots, 8$) and their values are $-0.3162230E+1$, $0.1875943E+1$, $-0.3859840E+0$, $0.1228261E+0$, $-0.4233006E-1$, $0.1379639E-1$, $-0.3846673E-2$, $0.8026637E-3$, and $-0.9257725E-4$, respectively. At points R and Q, $\beta = b$ and $\beta = B$. At points P and Q, $|\varepsilon|$ have the same value.

A nearly globally optimal FD scheme based on 2D time-space-domain dispersion relation

For 2D acoustic FD modeling, time-space-domain dispersion-relation-based spatial FD coefficients can be determined by adopting the following formula (Liu and Sen, 2009c):

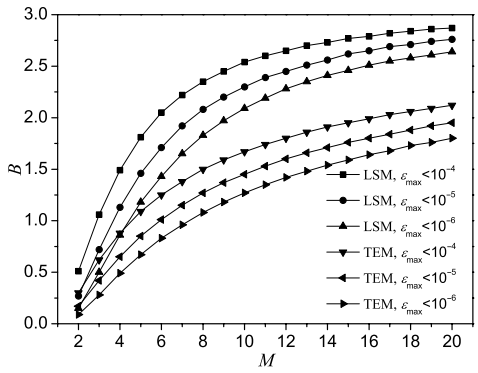

Figure 7. Variations of B with M for different maximum errors η by the TEM and the LSM of minimizing the relative error of space-domain dispersion relation, respectively: $\varepsilon_{\max} < \eta$ in the interval $[0, B]$.

Table 5. The b values used to calculate FD coefficients by the LSM of minimizing the relative error of space-domain dispersion relation for different M and maximum error η ($\varepsilon_{\max} < \eta$ in the interval $[0,B]$, B is shown in Table 4).

	b		
M	$\eta = 10^{-4}$	$\eta = 10^{-5}$	$\eta = 10^{-6}$
2	0.55	0.30	0.17
3	1.10	0.75	0.52
4	1.53	1.16	0.88
5	1.85	1.49	1.20
6	2.08	1.74	1.45
7	2.25	1.94	1.67
8	2.38	2.10	1.85
9	2.48	2.22	1.99
10	2.56	2.32	2.11
11	2.62	2.41	2.20
12	2.67	2.47	2.29
13	2.72	2.53	2.36
14	2.75	2.58	2.42
15	2.79	2.63	2.47
16	2.81	2.66	2.52
17	2.84	2.70	2.56
18	2.86	2.72	2.59
19	2.88	2.75	2.62
20	2.89	2.77	2.65
30	2.99	2.91	2.83
40	3.04	2.98	2.92
50	3.06	3.02	2.97

$$\sum_{m=1}^{M} c_m(2-\cos(mkh\,\cos\theta)-\cos(mkh\,\sin\theta)) \approx r^{-2}(1-\cos(rkh)), \tag{19}$$

where θ is the propagation direction angle of the plane wave.

Using TE for equation 19, FD coefficients can be obtained by solving the following equations (Liu and Sen, 2009c):

$$\sum_{m=1}^{M} m^{2j}(\cos^{2j}\theta+\sin^{2j}\theta)c_m = r^{2j-2}, \quad (j=1,2,\ldots,M). \tag{20}$$

I adopt $\theta = \pi/8$ to solve equations 20 to reach $(2M)$th-order accuracy along eight directions: $\theta = (2n-1)\pi/8$, $(n = 1, 2, \ldots, 8)$, and second-order accuracy along other directions (Liu and Sen, 2009c).

For 2D acoustic FD modeling, the relative error of phase velocity ξ is defined as follows (Liu and Sen, 2009c, 2011a):

$$\xi = \frac{v_{\mathrm{FD}}}{v} - 1 = \frac{2}{r\beta}\sin^{-1}\sqrt{\frac{r^2}{2}\sum_{m=1}^{M}(2-\cos(m\beta\cos\theta)-\cos(m\beta\sin\theta))c_m} - 1. \tag{21}$$

Similarly, I minimize the relative error between the left and right sides of equation 19. Then FD coefficients can be obtained by minimizing the square error over the given area $(0 \le \beta \le b, 0 \le \theta \le 2\pi)$ as the following:

$$\int_0^b \int_0^{2\pi} \left(\sum_{m=1}^{M} c_m\varphi_m(\beta,\theta) - 1\right)^2 d\theta d\beta, \tag{22}$$

where

$$\varphi_m(\beta,\theta) = \frac{2-\cos(m\beta\,\cos\theta)-\cos(m\beta\,\sin\theta)}{r^{-2}(1-\cos(r\beta))}. \tag{23}$$

Then, optimal c_m can be obtained by solving the following equations using LS:

$$\sum_{m=1}^{M}\left(\int_0^b\int_0^{2\pi}\varphi_m(\beta,\theta)\varphi_n(\beta,\theta)d\theta d\beta\right)c_m = \int_0^b\int_0^{2\pi}\varphi_n(\beta,\theta)d\theta d\beta, \quad (n=1,2,\ldots,M). \tag{24}$$

To examine the accuracy, I compute the variation of the maximum error $\xi_{\max}$ with b using the following formula:

$$\xi_{\max} = \max_{\beta\in[0,b],\theta\in[0,2\pi]}|\xi(\beta,\theta)|. \tag{25}$$

Considering periodicity and symmetry about θ, the range of θ can be reduced from $[0, 2\pi]$ to $[0, \pi/4]$.

Figure 13 shows variations of $\log_{10}(\xi_{\max})$ with b for different M by the TEM and the LSM of minimizing the relative error of 2D time-space-domain dispersion relation, respectively. This figure also demonstrates that the error increases with increasing b and increasing M, and the LSM has the larger wavenumber range than the TEM for the same maximum error. Figure 14 displays $\xi(\beta,\theta)$ by the TEM and the LSM of minimizing the relative error of 2D time-space-domain dispersion relation, respectively, where $M = 8$, $r = 0.15$. The value $b = 2.74$ is used in equation 24 together with 23 to calculate FD coefficients c_m.

Table 6. Optimized FD coefficients by the LSM of minimizing the relative error of space-domain dispersion relation for maximum error $\eta = 10^{-5}$.

c	$M = 2$	$M = 3$	$M = 4$	$M = 5$	
c_0	$-0.2505149E+1$	$-0.2749712E+1$	$-0.2903117E+1$	$-0.3006445E+1$	
c_1	$0.1336769E+1$	$0.1520749E+1$	$0.1645351E+1$	$0.1734054E+1$	
c_2	$-0.8419414E-1$	$-0.1584582E+0$	$-0.2236606E+0$	$-0.2790810E+0$	
c_3		$0.1256566E-1$	$0.3265851E-1$	$0.5678219E-1$	
c_4			$-0.2790073E-2$	$-0.9394879E-2$	
c_5				$0.8621379E-3$	
c	$M = 6$	$M = 7$	$M = 8$	$M = 9$	$M = 10$
c_0	$-0.3076778E+1$	$-0.3126507E+1$	$-0.3162230E+1$	$-0.3187510E+1$	$-0.3206547E+1$
c_1	$0.1796858E+1$	$0.1842502E+1$	$0.1875943E+1$	$0.1899945E+1$	$0.1918204E+1$
c_2	$-0.3234789E+0$	$-0.3586232E+0$	$-0.3859840E+0$	$-0.4064938E+0$	$-0.4225858E+0$
c_3	$0.8104263E-1$	$0.1034272E+0$	$0.1228261E+0$	$0.1385138E+0$	$0.1514992E+0$
c_4	$-0.1913579E-1$	$-0.3060513E-1$	$-0.4233006E-1$	$-0.5296301E-1$	$-0.6249474E-1$
c_5	$0.3443490E-2$	$0.7927665E-2$	$0.1379639E-1$	$0.2007472E-1$	$0.2637196E-1$
c_6	$-0.3401326E-3$	$-0.1539261E-2$	$-0.3846673E-2$	$-0.6984780E-2$	$-0.1066631E-1$
c_7		$0.1643770E-3$	$0.8026637E-3$	$0.2063534E-2$	$0.3915625E-2$
c_8			$-0.9257725E-4$	$-0.4573252E-3$	$-0.1219872E-2$
c_9				$0.5625035E-4$	$0.2863976E-3$
c_{10}					$-0.3744830E-4$

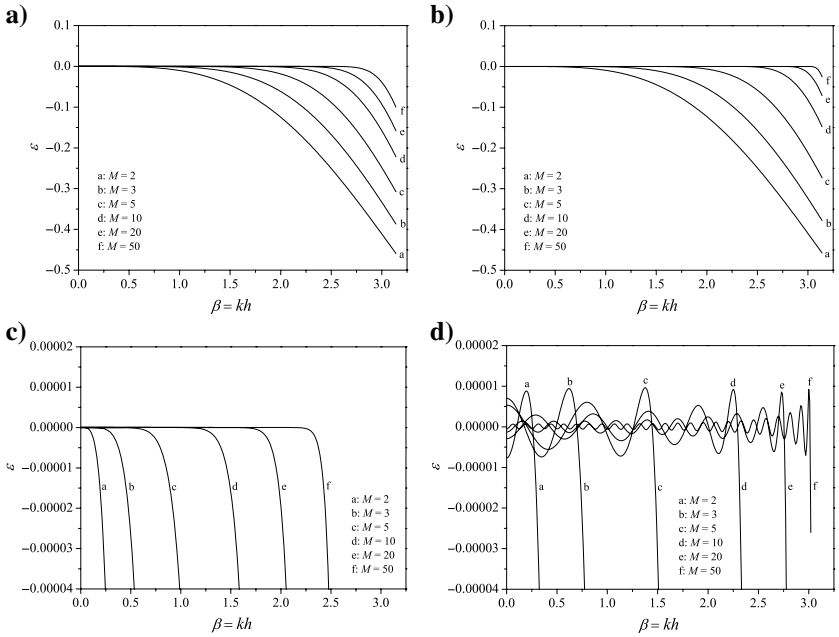

Figure 8. Variations of ε with β for different M by the TEM and the LSM of minimizing the relative error of space-domain dispersion relation, respectively: (a) by the TEM and (b) by the LSM. (c) Magnification of (a) and (d) Magnification of (b). FD coefficients of the LSM with maximum error $\eta = 10^{-5}$ used in the figure ($M = 2, 3, 5, 10$) are listed in Table 6.

For the given maximum error $\eta = 10^{-1.5}, 10^{-2.0}, 10^{-2.5}$, I obtain b values for different M from the TEM and the LSM shown in Figure 15, where $r = 0.15$, $\xi_{\max} < \eta$ is satisfied in the area $(0 \le \beta \le b, 0 \le \theta \le \pi/4)$ and b is used to calculate c_m. Figure 15 suggests that the LSM provides a much wider zone than the TEM for the same η and M. Figure 16 displays variations of $\zeta(\beta) = \max_\theta|\xi(\beta,\theta)|$ with β for different M from the TEM and the LSM, respectively. This figure shows that the LSM significantly widens the area with the given maximum error $\eta = 10^{-5}$ for the same M, compared to the TEM.

NUMERICAL EXAMPLES

I give three examples of 2D acoustic FD modeling for a homogeneous model, a large velocity-contrast model, and a heterogeneous model, respectively. These three modeling examples further demonstrate the accuracy and advantage of the proposed LS-based optimized spatial FD.

In this modeling scheme, I use the difference between the FD propagation time and the exact propagation time through one grid to describe FD error of acoustic modeling,

$$\delta = \frac{h}{v}((1+\xi)^{-1} - 1), \tag{26}$$

which is taken from Liu and Sen (2011a; equation 13).

For the given maximum frequency $f_{\max}$ and maximum error η, to obtain FD coefficients by the TEM and the LSM of minimizing the relative error of time-space-domain dispersion relation, the following inequality is satisfied:

$$|\delta(v, M, f)| \le \eta \quad \text{when } f \le f_{\max}, \tag{27}$$

which is from Liu and Sen (2011a; equation 15).

The first example is for a homogeneous model. Figure 17 displays snapshots and their differences of acoustic FD modeling for a homogeneous model using second-order temporal FD and $(2M)$th-order spatial FD from the TEM and the LSM of minimizing the relative error of the 2D time-space-domain dispersion relation, respectively. Modeling parameters are shown in the caption of Figure 17 and Table 7. Table 7 shows that the operator length can be decreased significantly when using the LSM, compared to the TEM, for the same modeling precision. From Figure 17, it can be seen that

- The modeling accuracy of the LSM with $M = 8$ (Figure 17d) is much greater than the TEM with $M = 8$ (Figure 17a),

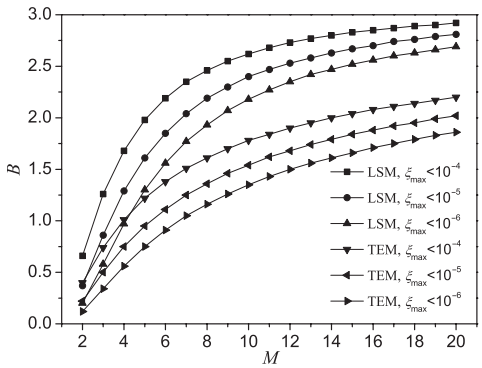

Figure 11. Variations of B with M and for different maximum errors η by the TEM and the LSM of minimizing the relative error of 1D acoustic time-space-domain dispersion relation, respectively. $r = 0.5$. $\xi_{\max} < \eta$ in the interval $[0, B]$.

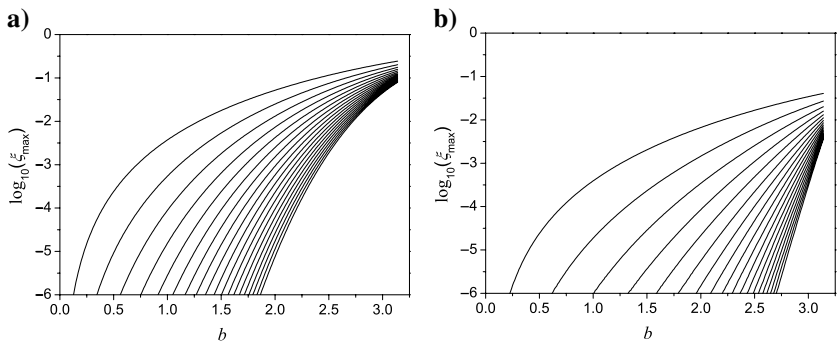

Figure 9. Variations of $\log_{10}(\xi_{\max})$ with b for different M by (a) the TEM and (b) the LSM of minimizing the relative error of 1D acoustic time-space-domain dispersion relation, respectively. From top to bottom, lines are from $M = 2, 3, \ldots, 20$, respectively. $r = 0.5$. Maximum values are calculated in the interval $[0, B]$.

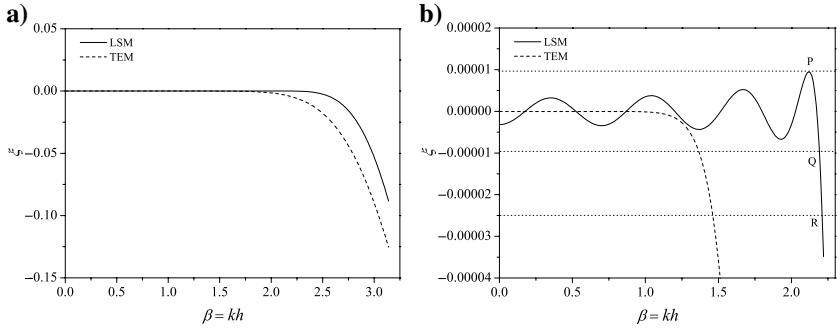

Figure 10. Variations of ξ with β (a) and its room (b) by the TEM and the LSM of minimizing the relative error of 1D acoustic time-space-domain dispersion relation, respectively: $M = 8$; $r = 0.5$. For the LSM, $b = 2.21$ is used in equation 8 together with 17 to calculate c_m $(m = 0, 1, \ldots, 8)$ and their values are $-0.2832397E{+}1$, $0.1624895E{+}1$, $-0.2721060E{+}0$, $0.8597278E{-}1$, $-0.3052312E{-}1$, $0.1046573E{-}1$, $-0.3127551E{-}2$, $0.7121103E{-}3$, and $-0.9074183E{-}4$, respectively. At points R and Q, $\beta = b$ and $\beta = B$. At points P and Q, $|\xi|$ have the same value.

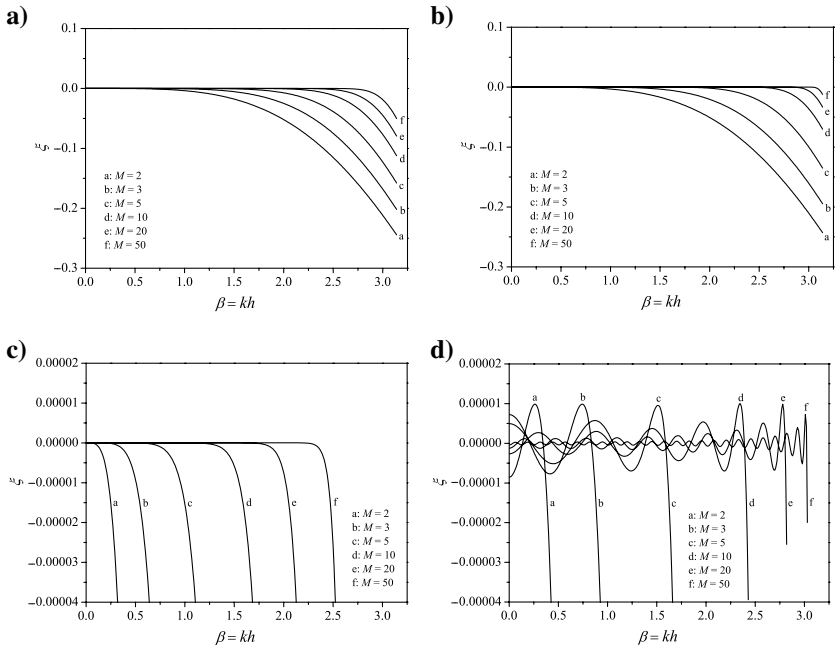

Figure 12. Variations of ξ with β for different M by the TEM and the LSM of minimizing the relative error of 1D acoustic time-space-domain dispersion relation, respectively: (a) by the TEM and (b) by the LSM. (c) Magnification of (a) and (d) is magnification of (b). The value of r is 0.5. FD coefficients of the LSM with $\eta = 10^{-5}$ are used in the figure.

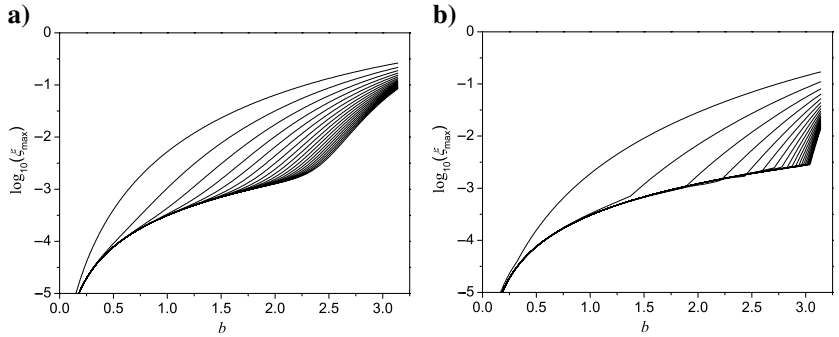

Figure 13. Variations of $\log_{10}(\xi_{max})$ with b for different M by minimizing the relative error of the 2D acoustic time-space-domain dispersion relation using (a) the TEM and (b) the LSM, respectively. From top to bottom, lines are from $M = 2$, 3, ..., 20, respectively. The value of r is 0.15. Maximum values are calculated in the area $(0 \le \beta \le b,\ 0 \le \theta \le \pi/4)$.

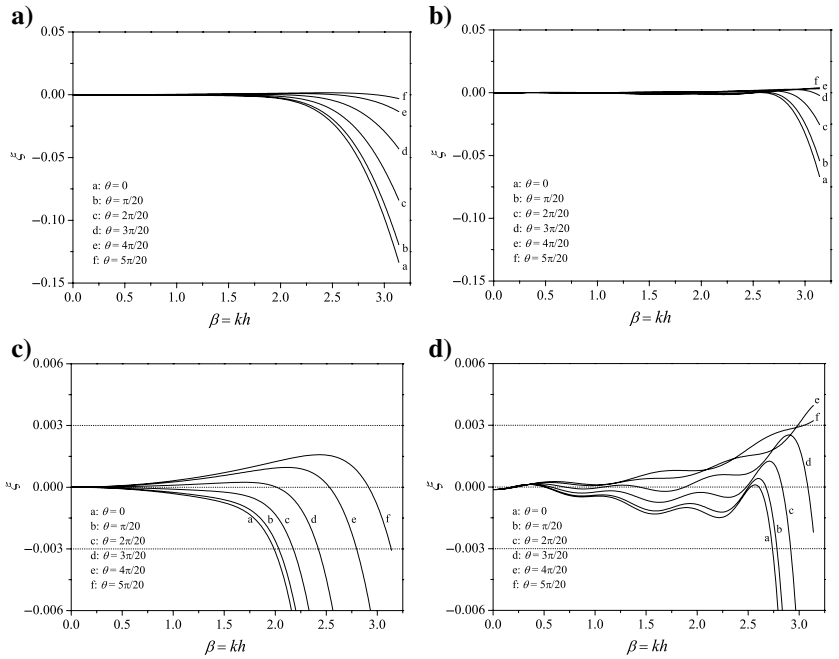

Figure 14. Variations of ξ with β for different θ by minimizing the relative error of 2D acoustic time-space-domain dispersion relation using the TEM and the LSM, respectively: (a) by the TEM and (b) by the LSM. (c) Magnification of (a) and (d) magnification of (b); $M = 8$ and $r = 0.15$. For the LSM, $b = 2.74$ is used in equation 24 together with 23 to calculate c_m ($m = 0, 1, \ldots, 8$) and their values are $-0.3190811E + 1$, $0.1911319E + 1$, $-0.4295264E + 0$, $0.1629466E + 0$, $-0.7193083E - 1$, $0.3265182E - 1$, $-0.1396133E - 1$, $0.4854164E - 2$, and $-0.9474453E - 3$, respectively.

and is nearly the same as the TEM with $M = 30$ (Figure 17b).

- The LSM with $M = 14$ (Figure 17e) has greater accuracy than the LSM with $M = 8$ (Figure 17d), slighter greater than the TEM with $M = 60$ (Figure 17c).

The second example is for a large velocity-contrast model with two layers. Figure 18 displays acoustic FD modeling snapshots by the reference solution, the TEM, and the LSM, and differences between the reference solution and the LSM. Modeling parameters are shown in the caption of Figure 18. Comparing Figure 18c to 18b, one can see that the LSM adopts the shorter spatial FD operator for the second layer but provides greater modeling accuracy.

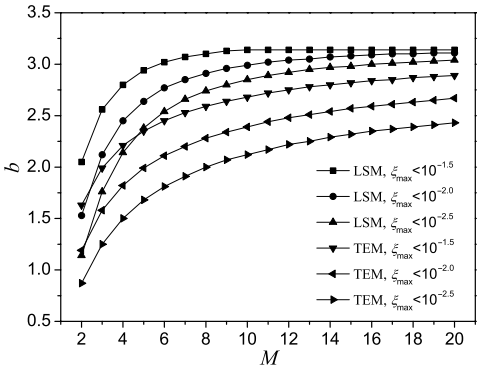

Figure 15. Variations of b for different M and given errors by minimizing the relative error of the 2D acoustic time-space-domain dispersion relation using the TEM and the LSM, respectively. $r = 0.15$. $\xi_{max} < \eta$ in the area $(0 \le \beta \le b, \quad 0 \le \theta \le \pi/4)$, $\eta = 10^{-1.5}$, $10^{-2.0}$, $10^{-2.5}$.

Figure 18c and 18a suggests that the modeling result of the LSM is quite close to the reference solution, and their differences shown in Figure 18d are very small. This modeling example demonstrates that the LS-based FD method is suitable for large velocity-contrast modeling.

The last example is for a heterogeneous model. Figure 19 shows the velocity model, snapshots, records, and their differences for the SEG/EAGE salt model. When using inequality 27 to design spatial FD operators, variable-length spatial operators are involved (Liu and Sen, 2011a). Hybrid absorbing boundary conditions are adopted for four boundaries (Liu and Sen, 2010) using 10 grid points for absorbing boundary reflections. Figure 19 demonstrates that the LSM can adopt a much shorter FD operator and thus is more computationally efficient than the TEM. Table 8 and Figure 20 display variations of FD operator length for different accuracies and methods, and they suggest that the LSM adopts much shorter FD operators and thus costs less computational time than the TEM. For 4000 time-step modeling of 600×200 grids, the CPU time on the same laptop computer is 957, 285, 143, 79, and 68 s, respectively, for the TEM with $M = 60$, the TEM with $M = 34$, the TEM with M from 34 to 3, the LSM with M from 14 to 2, and the LSM with M from 8 to 2.

It should be noted that spatial FD coefficients can be precomputed, and a little time will be taken to compute FD coefficients compared to wave-equation forward modeling. If a model has several different velocities, one can calculate FD coefficients for each velocity. When the model has many different velocities, to save memory for storing FD coefficients, one may calculate FD coefficients for some specified velocities with the same given small interval. To reduce the computational cost, I calculate FD coefficients for each specified velocity from the maximum velocity to the minimum velocity. Considering the FD operator length generally increases with decreasing velocity, when searching the optimal FD

Figure 16. Variations of $\zeta(\beta) = \max_\theta|\xi(\beta,\theta)|$ with β for different M by minimizing the relative error of 2D acoustic time-space-domain dispersion relation using the TEM and the LSM, respectively: (a) by the TEM and (b) by the LSM. (c) Magnification of (a) and (d) magnification of (b). The value of r is 0.15. FD coefficients of the LSM with $\eta = 10^{-2.5} \approx 0.003$ used in the figure.

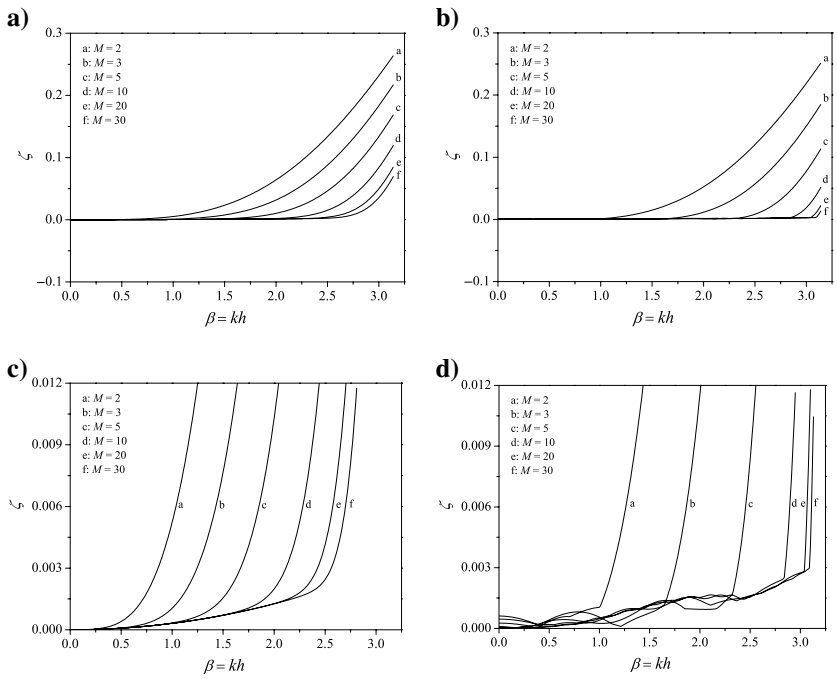

operator length for current velocity, the minimum searching length can be set as the length of the previous larger velocity and generally the optimal FD operator length for each velocity can be obtained after only a few times searching. For example, for the SEG/EAGE salt model, velocities change from 1500 to 4481 m/s. I calculate FD coefficients from the maximum velocity to the minimum velocity with an interval of 1 m/s, one time searching for most and two times searching for a few can find the optimal length of the LS-based FD operator for each velocity involved, and only about 1496 searching times are involved. Here, $f_{max} = 30$ Hz, $\eta = 10^{-5}$, the minimum of N is set as 2, and the searching time is defined as the time of solving equations 24 and 25. Considering characteristics of variations of FD operator length with velocity shown in Figure 19a, it is suitable to use the bisection method to obtain FD operator length for each velocity. When adopting the bisection

Table 7. The 2D spatial FD operator lengths $2M + 1$ by the TEM and the LSM for $v = 1500$ m/s, $h = 20$ m, and $\tau = 1$ ms.

		M from different methods	
f_{max} (Hz)	η	TEM	LSM
25.0	10^{-5}	14	6
30.0	10^{-5}	34	8
32.5	10^{-5}	60	11
34.0	10^{-5}	/	14

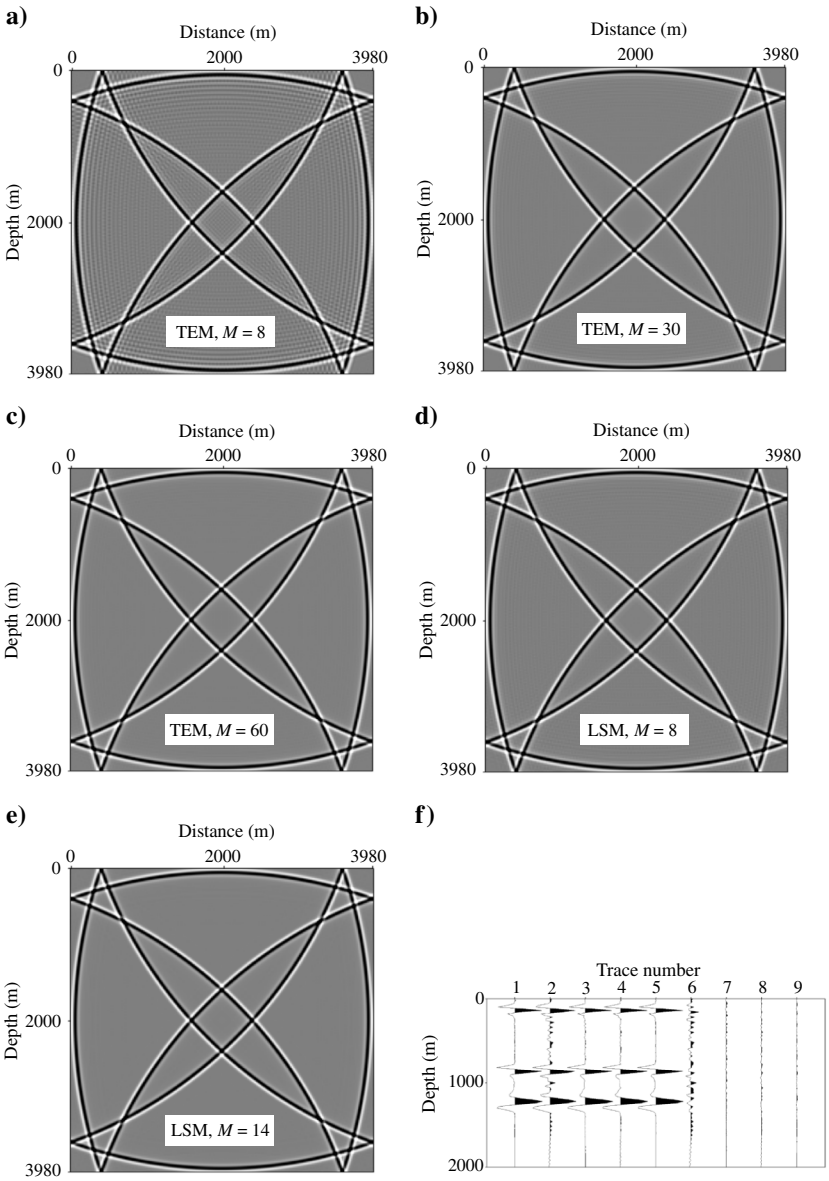

Figure 17. Snapshots at $t = 4.0$ s and their differences of acoustic FD modeling for a homogeneous model using second-order temporal FD and $(2M)$th-order spatial FD from the TEM and the LSM of minimizing the relative error of 2D time-space-domain dispersion relation, respectively. $v = 1500$ m/s, h=20m, $\tau = 1$ ms. Ricker wavelet with main frequency of 20 Hz, located in the center of the model, is used to generate vibrations. (a-c) Are by the TEM with $M = 8$, 30, and 60, respectively. (d, e) Are by the LSM with $M = 8$ and 14, respectively. (f) Shows comparisons of some traces from (a) to (e), traces 1, 2, 3, 4, and 5 with x coordinate of 1000 m are from (c, a, b, d, and e), respectively, Traces 6, 7, 8, and 9 are the differences between 2, 3, 4, 5, and 1, respectively.

method and the strategy of setting the minimum searching length for current velocity as the length of the previous larger velocity, only about 94 times of searching can find FD operator lengths for all 2982 different specified velocities of the SEG/EAGE salt model. Thus, it really costs quite a little computational time to get optimal FD operator lengths.

DISCUSSION

In this section, to further demonstrate the advantage of the proposed method, I develop LS-based algorithms to calculate optimal FD coefficients for two FD stencils, and I compare my results with published results (Yang and Balanis, 2006; Zhou and Zhang, 2011) through dispersion analysis.

Optimal FD coefficients for the compact FD stencil

To compare to the method by Zhou and Zhang (2011), I develop the LS-based algorithm to calculate optimal compact FD coefficients for second-order derivatives in Appendix C.

I adopt the same parameter $b = 0.9\pi$ used by Zhou and Zhang (2011) to calculate optimal FD coefficients and obtain

$$\begin{aligned} c_1 &= 1.934382E-1,\\ c_2 &= 4.389556E-1,\\ c_3 &= 2.057959E-2,\\ d_1 &= 5.095493E-1,\\ d_2 &= 5.768925E-2. \end{aligned} \tag{28}$$

The FD coefficients by Zhou and Zhang (2011; equation 14) are

$$\begin{aligned} c_1 &= 2.038930E-1,\\ c_2 &= 4.370825E-1,\\ c_3 &= 1.889244E-2,\\ d_1 &= 5.057370E-1,\\ d_2 &= 5.538830E-2. \end{aligned} \tag{29}$$

To compare these two methods, I calculate errors using formula C-1. Errors of the LSM and their method are $2.082684E-6$ and $1.217606E-5$, respectively. I also calculate errors using

$$\int_0^b \varepsilon^2(\beta)d\theta, \tag{30}$$

where

$$\varepsilon(\beta) = \frac{2\sum_{m=1}^{3}(1-\cos(m\beta))c_m}{1+2\sum_{m=1}^{2}d_m\cos(m\beta)} - \beta^2. \tag{31}$$

Errors are $4.649776E-5$ and $3.834470E-4$, respectively. The LSM has smaller errors in the given range $[0, b]$, which can be observed from Figure 20.

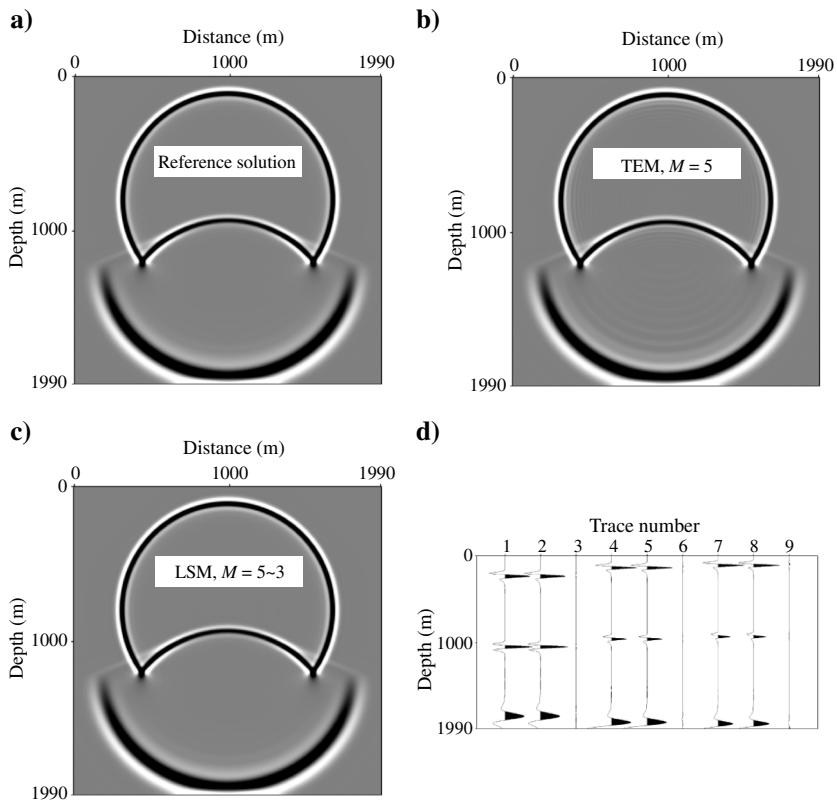

Figure 18. Snapshots at $t = 0.5$ s and their differences of acoustic FD modeling for a large velocity-contrast model. The model has two layers, $v_1 = 1500$ m/s, $v_2 = 4000$ m/s, the interface depth is 1200 m, $h = 10$ m. Second-order temporal FD is used in modeling. Ricker wavelet with main frequency of 25 Hz, located at (1000, 800 m), is used to generate vibrations. (a) Reference solution calculated by conventional 20th-order spatial FD and a small time step $\tau = 0.2$ ms. (b, c) Are modeled by $(2M)$th-order spatial FD from the TEM and the LSM of minimizing the relative error of 2D time-space-domain dispersion relation, respectively, $\tau = 1$ ms. (b) Is by the TEM with $M = 5$. (c) Is by the LSM, $f_{\max} = 50$ Hz, $M = 5$ for 1500 m/s and $M = 3$ for 4000 m/s. In figure (c), c_m $(m = 0, 1, \ldots, 5)$ for 1500 m/s are $-0.305033E+01$, $0.177768E+01$, $-0.315476E+0$, $0.772781E-01$, $-0.163274E-01$, $0.200462E-2$. c_m $(m = 0, 1, \ldots, 3)$ for 4000 m/s are $-0.290467E+1$, $0.164875E+1$, $-0.223818E+0$, and $0.274017E-1$. (d) Comparisons of some traces from (a) and (c). Traces 1, 4, and 7 are from (a), 2, 5, and 8 from (c). The x-coordinates of traces 1 and 2, 4 and 5, and 7 and 8 are 600, 800, and 1000 m, respectively. Traces 3, 6, and 9 are the difference between 1 and 2, 4 and 5, and 7 and 8, respectively.

Optimal FD coefficients for the FD stencil FD24-1

To compare to the method by Yang and Balanis (2006), I derive the LS-based algorithm to compute optimal FD coefficients for the FD stencil FD24-1 in Appendix D.

When $N_0 = 10$ and $r = 0.5$, optimal FD coefficients from the LSM are

$$c_1 = 1.08867864579431,$$
$$c_2 = -0.02955954859810, \quad (32)$$

and optimal FD coefficients from Yang and Balanis (2006; Table 1) are

Table 8. The 2D spatial FD operator lengths $2M + 1$ by the TEM and the LSM for v from 1500 to 4481 m/s, $h = 20$ m, and $\tau = 1$ ms.

		M from different methods	
f_{max} (Hz)	η	TEM	LSM
25.0	10^{-5}	$14 \sim 3$	$6 \sim 2$
30.0	10^{-5}	$34 \sim 3$	$8 \sim 2$
32.5	10^{-5}	$60 \sim 3$	$11 \sim 2$
34.0	10^{-5}	/	$14 \sim 2$

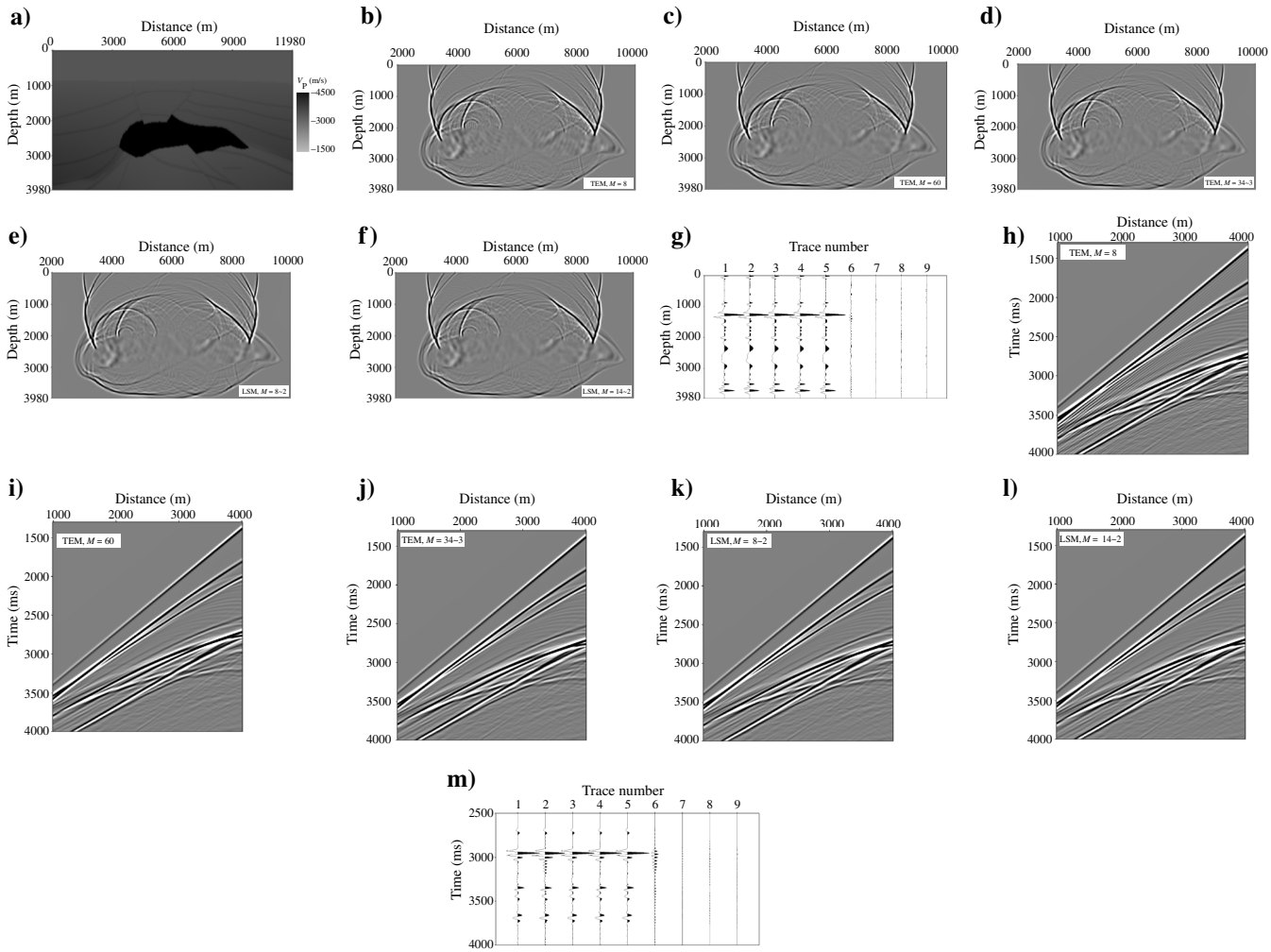

Figure 19. The 2D velocity model, modeling snapshots at $t = 1.6$ s, and records computed by the TEM and the LSM of minimizing the relative error of the 2D time-space-domain dispersion relation, respectively, with fixed FD operator lengths and with variable FD operator lengths for the SEG/EAGE salt model (a) ($h = 20$ m, $\tau = 1$ ms). Variable FD operator lengths are shown in Table 8. The source is located at (6000 m, 20 m). A Ricker wavelet with main frequency of 20 Hz is used to generate vibration. The depth of the receivers is 0 m. Hybrid absorbing boundary conditions are adopted for four boundaries, and the absorbing boundary layer has a thickness of 10 grids. (b-f) Are snapshots. (h-k and l) Are records. (b, h) Are by the TEM with $M = 8$. (c, i) Are by the TEM with $M = 60$. (d, j) Are by the TEM with M from 34 to 3. (e, k) Are by the LSM with M from 8 to 2. (f, l) Are by the LSM with M from 14 to 2. (g) Shows comparisons of some traces from (b-f); traces 1, 2, 3, 4, and 5 with an x-coordinate of 4000 m are from (c, b, d, e, f), respectively, Traces 6, 7, 8, and 9 are the differences between 2, 3, 4, 5, and 1, respectively. (m) Displays comparisons of some traces from (h-l); traces 1, 2, 3, 4, and 5 with an x-coordinate of 2000 m are from (i, h, j, k, l), respectively. Traces 6, 7, 8, and 9 are the differences between 2, 3, 4, 5, and 1, respectively.

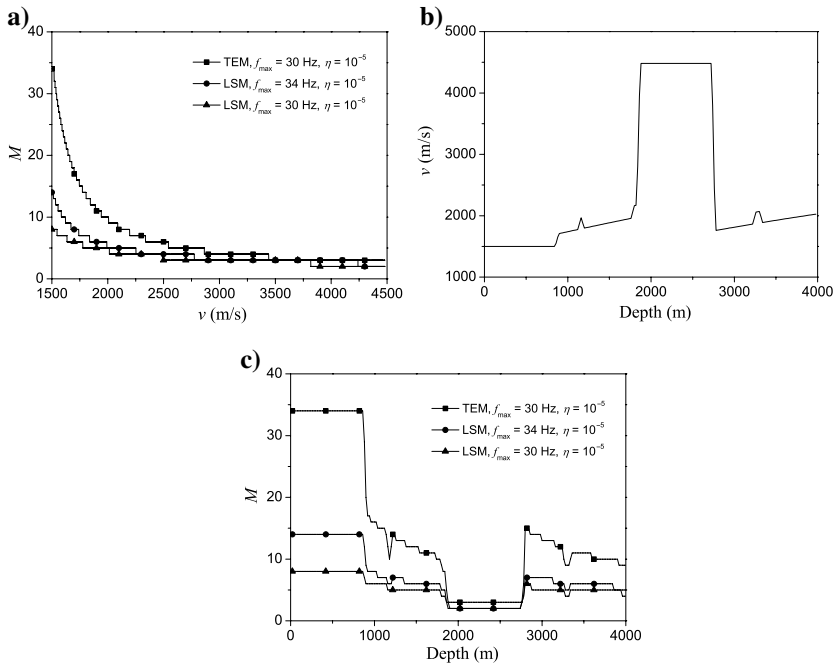

Figure 20. Variable FD operator lengths used in Figure 19. (a) Variation of M with velocity. (b) Variation of velocity with z at $x = 6000$ m. (c) Variation of M with z at $x = 6000$ m.

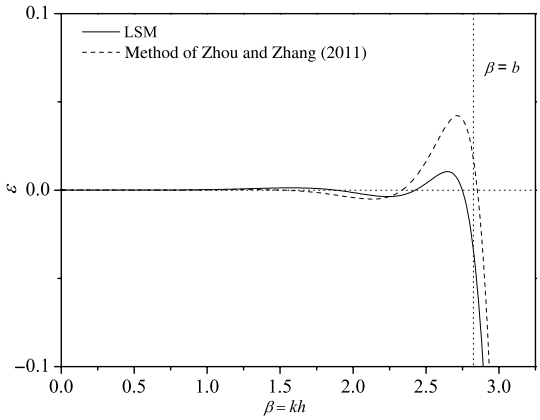

Figure 21. Variations of ε with β by the LSM and the method of Zhou and Zhang (2011) for the compact FD stencil. The value of ε is calculated by equation 31. The FD coefficients used are from equations 28 and 29, respectively.

$$c_1 = 1.08884578446620,$$
$$c_2 = -0.02961526148873. \quad (33)$$

To compare these two methods, I calculate errors using formula D-1. Errors of the LSM and their method are $6.038412E-8$ and $6.040010E-8$, respectively. I compute variations of error with propagation angle using

$$\varepsilon = f_0(\theta) + f_1(\theta)c_2 + f_2(\theta)c_2^2 - Q. \quad (34)$$

Figure 21 shows variations of $|\varepsilon|$ with β by the LSM and the method of Yang and Balanis (2006). Figure 22 shows variations of $|\varepsilon|$ with θ by the LSM and the method of Yang and Balanis (2006). It can be seen that the maximum error of the LSM is slightly smaller.

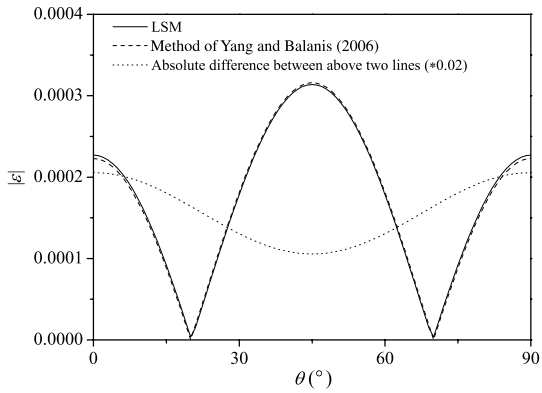

Figure 22. Variations of $|\varepsilon|$ with θ by the LSM and the method of Yang and Balanis (2006) for the FD stencil FD24-1. The value of $|\varepsilon|$ is calculated by equation 34. The FD coefficients used are from equations 32 and 33, respectively.

CONCLUSIONS

I have developed a new LS-based method to obtain FD coefficients. Globally optimal FD coefficients can be easily determined when the spatial FD operator length parameter M and the maximum error η are given. Compared with the conventional TE-based FD coefficients, LS-based coefficients provide a wider wavenumber range with the given maximum error for the same spatial FD operator length. Furthermore, I develop schemes to obtain LS-based optimal spatial FD coefficients by minimizing the relative error of space-domain dispersion relation for second-order derivatives, and time-space-domain dispersion relation for acoustic wave

equations. Accuracy analyses and modeling examples prove the advantages of the proposed method. Although the proposed method is for the second-order, it is suitable for first-order spatial derivatives on normal and staggered grids and similar problems.

ACKNOWLEDGMENTS

I thank the assistant editor J. Carcione, the associate editor S. Hestholm, and four anonymous reviewers for constructive criticism of my paper. This research is supported by National Nature Science Foundation of China (NSFC) under contract number 41074100 and by the Program for New Century Excellent Talents in the University of Ministry of Education of China under contract number NCET-10-0812.

APPENDIX A

WHY MINIMIZING THE RELATIVE ERROR IS PREFERABLE

In this appendix, first, I derive relative errors of phase velocity for acoustic FD modeling by minimizing the absolute error and the relative error of space-domain dispersion relation, respectively. Then, I explain why minimizing the relative error of space-domain dispersion relation is preferable to minimizing the absolute error for acoustic FD modeling. As an example, I only discuss the 1D case.

The relative error of the phase velocity by minimizing the relative error of the space-domain dispersion relation

In the given appropriate interval $[0, b]$, FD coefficients c_m derived by minimizing formula 7 using $\varphi_m(\beta)$ and $f(\beta)$ of equation 6 can generate the following equation:

$$2\sum_{m=1}^{M}(1-\cos(m\beta))c_m-\beta^2=\varepsilon, \tag{A-1}$$

where ε is small in the interval $[0, b]$.

Substitute equation A-1 into 16 and obtain the relative error of phase velocity,

$$\xi=\frac{2}{r\beta}\sin^{-1}\sqrt{r^2(\beta^2+\varepsilon)/4}-1. \tag{A-2}$$

Use TE and get

$$\frac{2}{r\beta}\sin^{-1}\sqrt{r^2(\beta^2+\varepsilon)/4}=\frac{2}{r\beta}\sin^{-1}(r\beta/2)+\frac{1}{\beta^2\sqrt{4-r^2\beta^2}}\varepsilon+O(\varepsilon^2), \tag{A-3}$$

where $O(\varepsilon^2)$ is the second-order infinitesimal about ε.

Substitute equation A-3 into A-2 and generate

$$\xi\approx\frac{2}{r\beta}\sin^{-1}(r\beta/2)-1+\frac{1}{\beta^2\sqrt{4-r^2\beta^2}}\varepsilon. \tag{A-4}$$

The relative error of the phase velocity by minimizing the relative error of the space-domain dispersion relation

Similarly, minimizing formula 7 using $\varphi_m(\beta)$ and $f(\beta)$ of equation 13 can give the following equation:

$$\frac{2\sum_{m=1}^{M}(1-\cos(m\beta))c_m}{\beta^2}-1=\varepsilon. \tag{A-5}$$

Substitute equation A-5 into 16 and generate

$$\xi=\frac{2}{r\beta}\sin^{-1}\sqrt{r^2\beta^2(1+\varepsilon)/4}-1. \tag{A-6}$$

Use TE and obtain

$$\frac{2}{r\beta}\sin^{-1}\sqrt{r^2\beta^2(1+\varepsilon)/4}=\frac{2}{r\beta}\sin^{-1}(r\beta/2)+\frac{1}{\sqrt{4-r^2\beta^2}}\varepsilon+O(\varepsilon^2). \tag{A-7}$$

Substitute equation A-7 into A-6 and get

$$\xi\approx\frac{2}{r\beta}\sin^{-1}(r\beta/2)-1+\frac{1}{\sqrt{4-r^2\beta^2}}\varepsilon. \tag{A-8}$$

Comparing formula A-8 with A-4, one can find that A-4 generates a large error while the wavenumber is close to zero. To decrease modeling errors for small wavenumbers, optimal FD coefficients are suggested to be designed by minimizing the relative wavenumber error in numerical wave equations.

APPENDIX B

MINIMIZING RELATIVE ERROR OF TIME-SPACE-DOMAIN DISPERSION RELATION LEADS TO SMALL RELATIVE ERROR OF PHASE VELOCITY

In this appendix, I explain why minimizing the relative error of time-space-domain dispersion relation for acoustic FD modeling can lead to the small relative error of phase velocity and the small FD error. As an example, I also only discuss the 1D case.

In the given appropriate interval $[0, b]$, FD coefficients c_m derived by minimizing formula 7 using $\varphi_m(\beta)$ and $f(\beta)$ of equation 17 can generate the following equation:

$$\sum_{m=1}^{M} \frac{1-\cos(m\beta)}{r^{-2}(1-\cos(r\beta))} c_m - 1 = \varepsilon, \tag{B-1}$$

where ε is small in the interval $[0, b]$.

Then,

$$\frac{1}{2}\sum_{m=1}^{M} r^2(1-\cos(m\beta))c_m = \sin^2(r\beta/2)(1+\varepsilon). \tag{B-2}$$

Substitute equation B-2 into 16 and obtain

$$\xi = \frac{2}{r\beta}\sin^{-1}(\sin(r\beta/2)(1+\varepsilon)^{1/2}) - 1. \tag{B-3}$$

Use TE and get

$$\frac{2}{r\beta} sin^{-1}(\sin(r\beta/2)(1+\varepsilon)^{1/2}) = 1 + \frac{\tan(r\beta/2)}{r\beta}\varepsilon + O(\varepsilon^2), \tag{B-4}$$

where $O(\varepsilon^2)$ is the second-order infinitesimal about ε.

Substitute equation B-4 into B-3 and generate

$$\xi \approx \frac{\tan(r\beta/2)}{r\beta}\varepsilon. \tag{B-5}$$

This formula suggests that the relative error of the phase velocity is small in the interval $[0, b]$. Comparing equation B-5 to A-8, one can find that B-5 generally provides much less error than A-8 because ε is small and $\tan(r\beta/2)/r\beta < 1/\sqrt{4 - r^2\beta^2}$ when $0 < r\beta < 2$, which demonstrates that minimizing the relative error of time-space-domain dispersion relation leads to the smaller error than minimizing the relative error of the space-domain dispersion relation for acoustic FD modeling.

Using equation B-5, equation 26 can be approximately expressed as follows:

$$\delta = \frac{h}{v}((1+\xi)^{-1} - 1) \approx -\frac{h}{v}\xi \approx -\frac{h\tan(r\beta/2)}{vr\beta}\varepsilon. \tag{B-6}$$

This formula also shows that the FD error of acoustic modeling δ is also small in the interval $[0, b]$.

APPENDIX C

LS-BASED OPTIMAL ALGORITHM FOR THE COMPACT FD STENCIL

In this appendix, to compare my method to the method by Zhou and Zhang (2011); as an example, I derive the LS-based algorithm to calculate optimal compact FD coefficients for second-order derivatives.

From Zhou and Zhang (2011; equations 10–12), I get the square error over the given interval $[0, b]$ as follows:

$$E = \int_0^b \left(2\sum_{m=1}^{3}(1-\cos(m\beta))c_m - \left(1+2\sum_{m=1}^{2} d_m\cos(m\beta)\right)\beta^2\right)^2 d\theta, \tag{C-1}$$

where c_m and d_m are FD coefficients.

Satisfying the constraint equations from Zhou and Zhang (2011; equations 5 and 6), I have

$$1 + 2d_1 + 2d_2 = c_1 + 4c_2 + 9c_3, \tag{C-2}$$

$$12d_1 + 48d_2 = c_1 + 16c_2 + 81c_3. \tag{C-3}$$

Then,

$$d_m = q_{m,0} + \sum_{l=1}^{3} q_{m,l}c_l, \qquad (m = 1, 2), \tag{C-4}$$

where $q_{1,0}$, $q_{1,1}$, $q_{1,2}$, and $q_{1,3}$ are $-2/3$, $23/36$, $20/9$, $15/4$, respectively; $q_{2,0}$, $q_{2,1}$, $q_{2,2}$, and $q_{2,3}$ are $1/6$, $5/36$, $2/9$, $3/4$, respectively.

Substitute equation C-4 into C-1 and obtain formula 7 with $M = 3$ and

$$\varphi_m(\beta) = 2(1-\cos(m\beta)) - 2\sum_{l=1}^{2} q_{l,m}\cos(l\beta)\beta^2, \quad (m = 1, 2, 3), \tag{C-5}$$

$$f(\beta) = \left(1 + 2\sum_{l=1}^{N} q_{l,0}\cos(l\beta)\right)\beta^2. \tag{C-6}$$

Compact FD coefficients c_m can be obtained by minimizing formula 7 in which $\varphi_m(\beta)$ and $f(\beta)$ are replaced by equations C-5 and C-6. Then, compact FD coefficients d_m can be determined by equation C-4.

APPENDIX D

LS-BASED OPTIMAL ALGORITHM FOR THE FD STENCIL FD24-1

In this appendix, to compare my method to the method by Yang and Balanis (2006), as an example, I derive the LS-based optimal algorithm for the FD stencil FD24-1.

From Yang and Balanis (2006; equations 2, 4, and 5), I get the square error over the given interval $[0, \pi/2]$ as follows:

$$E = \int_0^{\pi/2} [f_0(\theta) + f_1(\theta)c_2 + f_2(\theta)c_2^2 - Q]^2 d\theta, \tag{D-1}$$

where

$$f_0(\theta) = (u_1(\theta))^2 + (w_1(\theta))^2, \tag{D-2}$$

$$f_1(\theta) = 2(u_1(\theta)u_2(\theta) + w_1(\theta)w_2(\theta)), \tag{D-3}$$

$$f_2(\theta) = ((u_2(\theta))^2 + (w_2(\theta))^2), \tag{D-4}$$

$$u_1(\theta) = \sin\left(\frac{\pi \cos\theta}{N_0}\right), \tag{D-5}$$

$$u_2(\theta) = \sin\left(\frac{3\pi \cos\theta}{N_0}\right) - 3\sin\left(\frac{\pi \cos\theta}{N_0}\right), \tag{D-6}$$

$$w_1(\theta) = \sin\left(\frac{\pi \sin\theta}{N_0}\right), \tag{D-7}$$

$$w_2(\theta) = \sin\left(\frac{3\pi \sin\theta}{N_0}\right) - 3\sin\left(\frac{\pi \sin\theta}{N_0}\right), \tag{D-8}$$

$$Q = \frac{1}{r^2}\sin^2\left(\frac{\pi r}{N_0}\right), \tag{D-9}$$

where r is the Courant number, N_0 is the number of grids per wavelength, θ represents the propagation angle, c_1 and c_2 are FD coefficients, $c_1 = 1 - 3c_2$.

Minimizing the square error of formula D-1 by LS, I have

$$\xi_3 c_2^3 + \xi_2 c_2^2 + \xi_1 c_2 + \xi_0 = 0, \tag{D-10}$$

where

$$\xi_3 = \int_0^{\pi/2} 2(f_2(\theta))^2 d\theta, \tag{D-11}$$

$$\xi_2 = \int_0^{\pi/2} 3 f_1(\theta) f_2(\theta) d\theta, \tag{D-12}$$

$$\xi_1 = \int_0^{\pi/2} ((f_1(\theta))^2 + 2 f_0(\theta) f_2(\theta) - 2 Q f_2(\theta)) d\theta, \tag{D-13}$$

$$\xi_0 = \int_0^{\pi/2} (f_0(\theta) - Q) f_1(\theta) d\theta. \tag{D-14}$$

Solve equation D-10 and get three roots: c_2 equals the root providing the least error, and $c_1 = 1 - 3c_2$.

REFERENCES

Bansal, R., and M. K. Sen, 2008, Finite-difference modelling of S-wave splitting in anisotropic media: Geophysical Prospecting, **56**, 293–312, doi: 10.1111/j.1365-2478.2007.00693.x.

Chen, J., 2012, An average-derivative optimal scheme for frequency-domain scalar wave equation: Geophysics, **77**, no. 6, T201–T210, doi: 10.1190/geo2011-0389.1.

Chu, C., and P. L. Stoffa, 2012a, Implicit finite-difference simulations of seismic wave propagation: Geophysics, **77**, no. 2, T57–T67, doi: 10.1190/geo2011-0180.1.

Chu, C., and P. L. Stoffa, 2012b, Determination of finite-difference weights using scaled binomial windows: Geophysics, **77**, no. 3, W17–W26, doi: 10.1190/geo2011-0336.1.

Dablain, M. A., 1986, The application of high-order differencing to the scalar wave equation: Geophysics, **51**, 54–66, doi: 10.1190/1.1442040.

Du, Q., B. Li, and B. Hou, 2009, Numerical modeling of seismic wavefields in transversely isotropic media with a compact staggered-grid finite difference scheme: Applied Geophysics, **6**, 42–49, doi: 10.1007/s11770-009-0008-z.

Etgen, J. T., and M. J. O'Brien, 2007, Computational methods for large-scale 3D acoustic finite-difference modeling: A tutorial: Geophysics, **72**, no. 5, SM223–SM230, doi: 10.1190/1.2753753.

Finkelstein, B., and R. Kastner, 2007, Finite difference time domain dispersion reduction schemes: Journal of Computational Physics, **221**, 422–438, doi: 10.1016/j.jcp.2006.06.016.

Fornberg, B., 1987, The pseudospectral method — comparisons with finite differences for the elastic wave equation: Geophysics, **52**, 483–501, doi: 10.1190/1.1442319.

Fornberg, B., 1998, Calculation of weights in finite difference formulas: SIAM Review, **40**, 685–691, doi: 10.1137/S0036144596322507.

Hestholm, S., 2009, Acoustic VTI modeling using high-order finite differences: Geophysics, **74**, no. 5, T67–T73, doi: 10.1190/1.3157242.

Holberg, O., 1987, Computational aspects of the choice of operator and sampling interval for numerical differentiation in large-scale simulation of wave phenomena: Geophysical Prospecting, **35**, 629–655, doi: 10.1111/j.1365-2478.1987.tb00841.x.

Igel, H., P. Mora, and B. Riollet, 1995, Anisotropic wave propagation through finite-difference grids: Geophysics, **60**, 1203–1216, doi: 10.1190/1.1443849.

JafarGandomi, A., and H. Takenaka, 2009, Non-standard FDTD for elastic wave simulation: Two-dimensional P-SV case: Geophysical Journal International, **178**, 282–302, doi: 10.1111/j.1365-246X.2009.04101.x.

Jastram, C., and A. Behle, 1993, Accurate finite-difference operators for modelling the elastic wave equation: Geophysical Prospecting, **41**, 453–458, doi: 10.1111/j.1365-2478.1993.tb00579.x.

Kelly, K. R., R. Ward, W. S. Treitel, and R. M. Alford, 1976, Synthetic seismograms: A finite-difference approach: Geophysics, **41**, 2–27, doi: 10.1190/1.1440605.

Kindelan, M., A. Kamel, and P. Sguazzero, 1990, On the construction and efficiency of staggered numerical differentiators for the wave equation: Geophysics, **55**, 107–110, doi: 10.1190/1.1442763.

Kosloff, D., R. C. Pestana, and H. Tal-Ezer, 2010, Acoustic and elastic numerical wave simulations by recursive spatial derivative operators: Geophysics, **75**, no. 6, T167–T174, doi: 10.1190/1.3485217.

Leandro, D. B., C. Dors, and W. J. Mansur, 2012, A new family of finite-difference schemes to solve the heterogeneous acoustic wave equation: Geophysics, **77**, no. 5, T187–T199, doi: 10.1190/geo2011-0345.1.

Lele, S. K., 1992, Compact finite difference schemes with spectral-like resolution: Journal of Computational Physics, **103**, 16–42, doi: 10.1016/0021-9991(92)90324-R.

Levander, A. R., 1988, Fourth-order finite-difference P-SV seismograms: Geophysics, **53**, 1425–1436, doi: 10.1190/1.1442422.

Liu, Y., C. Li, and Y. Mou, 1998, Finite-difference numerical modeling of any even-order accuracy: Oil Geophysical Prospecting, **33**, 1–10, in Chinese, http://www.cqvip.com/qk/93077x/199801/3339195.html.

Liu, Y., and M. K. Sen, 2009a, A practical implicit finite-difference method: Examples from seismic modeling: Journal of Geophysics and Engineering, **6**, 231–249, doi: 10.1088/1742-2132/6/3/003.

Liu, Y., and M. K. Sen, 2009b, An implicit staggered-grid finite-difference method for seismic modeling: Geophysical Journal International, **179**, 459–474, doi: 10.1111/j.1365-246X.2009.04305.x.

Liu, Y., and M. K. Sen, 2009c, A new time-space domain high-order finite-difference method for the acoustic wave equation: Journal of Computational Physics, **228**, 8779–8806, doi: 10.1016/j.jcp.2009.08.027.

Liu, Y., and M. K. Sen, 2009d, Numerical modeling of wave equation by truncated high-order finite difference method: Earthquake Science, **22**, 205–213, doi: 10.1007/s11589-009-0205-0.

Liu, Y., and M. K. Sen, 2010, A hybrid scheme for absorbing edge reflections in numerical modeling of wave propagation: Geophysics, **75**, no. 2, A1–A6, doi: 10.1190/1.3295447.

Liu, Y., and M. K. Sen, 2011a, Finite-difference modeling with adaptive variable-length spatial operators: Geophysics, **76**, no. 4, T79–T89, doi: 10.1190/1.3587223.

Liu, Y., and M. K. Sen, 2011b, 3D acoustic wave modeling with time-space domain dispersion-relation-based finite-difference schemes and hybrid absorbing boundary conditions: Exploration Geophysics, **42**, 176–189, doi: 10.1071/EG11007.

Liu, Y., and X. Wei, 2008, Finite-difference numerical modeling with even-order accuracy in two-phase anisotropic media: Applied Geophysics, **5**, 107–114, doi: 10.1007/s11770-008-0014-6.

Moczo, P., J. Kristek, M. Galis, E. Chaljub, and V. Etienne, 2011, 3-D finite-difference, finite-element, discontinuous-Galerkin and spectral-element schemes analysed for their accuracy with respect to P-wave to S-wave speed ratio: Geophysical Journal International, **187**, 1645–1667, doi: 10.1111/j.1365-246X.2011.05221.x.

Moczo, P., J. Kristek, and L. Halada, 2000, 3D fourth-order staggered-grid finite-difference schemes: Stability and grid dispersion: Bulletin of the

Seismological Society of America, **90**, 587–603, doi: 10.1785/0119990119.
Robertsson, J. O. A., J. O. Blanch, W. W. Symes, and C. S. Burrus, 1994, Galerkin-wavelet modeling of wave propagation: Optimal finite difference stencil design: Mathematical and Computer Modelling, **19**, 31–38, doi: 10.1016/0895-7177(94)90113-9.
Saenger, E. H., N. Gold, and S. A. Shapiro, 2000, Modeling the propagation of elastic waves using a modified finite-difference grid: Wave Motion, **31**, 77–92, doi: 10.1016/S0165-2125(99)00023-2.
Shan, G., 2009, Optimized implicit finite-difference and Fourier finite-difference migration for VTI media: Geophysics, **74**, no. 6, WCA189–WCA197, doi: 10.1190/1.3202306.
Song, X., and S. Fomel, 2011, Fourier finite-difference wave propagation: Geophysics, **76**, no. 5, T123–T129, doi: 10.1190/geo2010-0287.1.
Takeuchi, N., and R. J. Geller, 2000, Optimally accurate second order time-domain finite difference scheme for computing synthetic seismograms in 2-D and 3-D media: Physics of the Earth and Planetary Interiors, **119**, 99–131, doi: 10.1016/S0031-9201(99)00155-7.
Tam, C. K. W., and J. C. Webb, 1993, Dispersion-relation-preserving finite difference schemes for computational acoustics: Journal of Computational Physics, **107**, 262–281, doi: 10.1006/jcph.1993.1142.
Virieux, J., 1984, *SH*-wave propagation in heterogeneous media: Velocity-stress finite-difference method: Geophysics, **49**, 1933–1957, doi: 10.1190/1.1441605.
Virieux, J., 1986, P-SV wave propagation in heterogeneous media: Velocity stress finite difference method: Geophysics, **51**, 889–901, doi: 10.1190/1.1442147.
Yang, B., and C. A. Balanis, 2006, Least square method to optimize the coefficients of complex finite-difference space stencils: IEEE Antennas and Wireless Propagation Letters, **5**, 450–453, doi: 10.1109/LAWP.2006.885012.
Zhang, J., and Z. Yao, 2012, Globally optimized finite-difference extrapolator for strongly VTI media: Geophysics, **77**, no. 4, T125–T135, doi: 10.1190/geo2011-0505.1.
Zhou, B., and S. A. Greenhalgh, 1992, Seismic scalar wave equation modeling by a convolutional differentiator: Bulletin of the Seismological Society of America, **82**, 289–303.
Zhou, H., and G. Zhang, 2011, Prefactored optimized compact finite-difference schemes for second spatial derivatives: Geophysics, **76**, no. 5, WB87–WB95, doi: 10.1190/geo2011-0048.1.